Molecular Microbiology (2014) 94(5), 1041–1064 ■
doi:10.1111/mmi.12813
First published online 27 October 2014

Staphylococcus aureus DivIB is a peptidoglycan-binding protein that is required for a morphological checkpoint in cell division

Amy L. Bottomley,† Azhar F. Kabli, Alexander F. Hurd, Robert D. Turner, Jorge Garcia-Lara and Simon J. Foster*
The Krebs Institute, Department of Molecular Biology and Biotechnology, University of Sheffield, Western Bank, Sheffield S10 2TN, UK.

Summary

Bacterial cell division is a fundamental process that requires the coordinated actions of a number of proteins which form a complex macromolecular machine known as the divisome. The membrane-spanning proteins DivIB and its orthologue FtsQ are crucial divisome components in Gram-positive and Gram-negative bacteria respectively. However, the role of almost all of the integral division proteins, including DivIB, still remains largely unknown. Here we show that the extracellular domain of DivIB is able to bind peptidoglycan and have mapped the binding to its β subdomain. Conditional mutational studies show that *divIB* is essential for *Staphylococcus aureus* growth, while phenotypic analyses following depletion of DivIB results in a block in the completion, but not initiation, of septum formation. Localisation studies suggest that DivIB only transiently localises to the division site and may mark previous sites of septation. We propose that DivIB is required for a molecular checkpoint during division to ensure the correct assembly of the divisome at midcell and to prevent hydrolytic growth of the cell in the absence of a completed septum.

Introduction

Cell division in bacteria requires the coordinated action of a number of proteins which form a complex macromolecular machine known as the divisome (Errington *et al.*, 2003). Many components of the divisome have been shown to be essential for viability: 10 genes involved in cell division are essential in *Bacillus subtilis* (Kobayashi *et al.*, 2003), *Escherichia coli* (Buddelmeijer and Beckwith, 2002) and *Caulobacter crescentus* (Goley *et al.*, 2011), while eight division genes are essential in *Streptococcus pneumoniae* (Song *et al.*, 2005; van Opijnen *et al.*, 2009). The tubulin homologue FtsZ is the most highly conserved of the division proteins, and FtsZ recruitment into the Z-ring at midcell is the first step in the division process. The Z-ring acts as a scaffold for the recruitment and assembly of subsequent essential and accessory divisome proteins. The divisome is composed of FtsZ-associated proteins (FtsA, ZapA, FtsE/X, [ZipA ZapB ZapC; *E. coli*], [EzrA, SepF; *B. subtilis*]), and membrane-spanning proteins (including FtsK, FtsW, FtsQ/DivIB, FtsL, FtsB/DivIC, FtsI/PBP2B, FtsN [*E. coli*]), many of which are involved in the biosynthesis of septal peptidoglycan (Errington *et al.*, 2003; Schmidt *et al.*, 2004; Ishikawa *et al.*, 2006; Ebersbach *et al.*, 2008).

While key components of the divisome, such as FtsZ, are highly conserved throughout bacterial species, others have diverged significantly (Angert, 2005). This diversity of cell division mechanisms carried out by the set of cell division proteins that comprise the divisome in each species is likely to be influenced by bacterial shape and envelope structures. Most studies of cell division have focused on the rod-shaped model organisms *E. coli* and *B. subtilis*. In rods, there are three phases of cell wall synthesis: elongation due to lateral peptidoglycan synthesis, involving MreB/Mbl (Daniel and Errington, 2003; Figge *et al.*, 2004); pre-septal elongation (Typas *et al.*, 2012) and septation due to FtsZ-driven peptidoglycan synthesis at the midcell (Errington *et al.*, 2003), with each process involving two distinct protein complexes. A comprehensive analysis of sequenced bacterial genomes found a correlation between a lack of *mreB* and non-rod shape, with exceptions of some cyanobacteria and the *Chlamydia* (Daniel and Errington, 2003). Using coccus-shaped bacteria to study cell division may therefore prove a simpler model due to the lack of cylindrical elongation of the cell wall and thus elimination of potential overlapping roles of cell wall synthesis machineries (Turner *et al.*, 2010).

Accepted 29 September, 2014. *For correspondence. E-mail s.foster@sheffield.ac.uk; Tel. (+44) 114 222 4411; Fax (+44) 114 272 8697. †Present address: The ithree Institute, University of Technology Sydney, Sydney, New South Wales 2007, Australia.

Indeed, the human pathogen *Staphylococcus aureus* does not undergo an elongation growth phase but instead synthesises peptidoglycan only at the septum in an FtsZ-dependent manner (Pinho and Errington, 2003), with the septum becoming the nascent hemispherical poles of the daughter cells following cleavage of the septal cell wall. Atomic Force Microscopy (AFM) has been used to study *S. aureus* peptidoglycan architecture and dynamics, and revealed a thickening of peptidoglycan, described as a 'piecrust', midcell at the site of the presumptive septum (Turner *et al*., 2010). After subsequent completion of the septum the piecrust remains as orthogonal 'ribs' due to hydrolytic turnover of the cell wall, marking the location of previous division planes.

Staphylococcus aureus is a close relative of *B. subtilis*, and homologues of all genes essential for vegetative division in *B. subtilis* are found to be conserved in *S. aureus* (Steele *et al*., 2011). Accordingly, while there is likely to be a conservation of the cell division process among prokaryotes, much can be learned from comparative studies of morphologically diverse bacteria. There is also a direct interest in studying cell division in coccus-shaped bacteria, as many species are prevalent human pathogens (e.g. *S. pneumoniae*, *S. aureus*, *Neisseria meningitidis*, *Neisseria gonorrhoeae*), and an understanding of cell growth and division in these bacteria may aid in the identification of novel antimicrobial targets.

While there is a degree of conservation of division proteins throughout bacterial species, differences in the essentiality of some of these proteins have been reported in different species. The *ftsQ* gene of *E. coli* is essential, with thermosensitive mutants forming aseptate filaments or filaments with partially formed septa when grown at the non-permissive temperature (Begg *et al*., 1980; Carson *et al*., 1991). In *B. subtilis*, *divIB* is only essential for vegetative growth at high temperatures but is required for sporulation at all temperatures (Beall and Lutkenhaus, 1989; Harry *et al*., 1993). *Streptomyces coelicolor divIB* is dispensable for mycelial growth but is necessary for sporulation septation to allow the conversion of aerial hyphae into spores (McCormick and Losick, 1996). In *S. pneumoniae*, *divIB* was found to be non-essential for growth in rich media, although deletion resulted in an altered morphology to longer chains that lysed earlier after the onset of stationary phase, and was essential for nutrient-limited growth (Le Gouellec *et al*., 2008). A recent large-scale transposon mutagenesis screen of *S. aureus* has suggested that *divIB* is essential for cell viability (Chaudhuri *et al*., 2009).

Although cell division has been well studied for many decades, the biochemical role of each of the membrane-spanning divisome proteins, with the exception of FtsI (Nguyen-Disteche *et al*., 1998) and FtsW (Mohammadi *et al*., 2011), is mostly unknown. A trimeric complex of DivIB, DivIC and FtsL in Gram-positives, and their orthologues FtsQ, FtsB and FtsL in Gram-negatives, is conserved in all species for which division protein interactions have been investigated, suggesting functional importance (Buddelmeijer and Beckwith, 2004; Noirclerc-Savoye *et al*., 2005; Daniel *et al*., 2006). There are strong interdependencies between DivIB, DivIC and FtsL for the stabilisation of this heterocomplex and recruitment to the division site, as well as midcell localisation of penicillin-binding protein (PBP) 2B (FtsI) (Daniel *et al*., 1998; 2000; 2006; Ghigo *et al*., 1999; Weiss *et al*., 1999; Daniel and Errington, 2000; Buddelmeijer *et al*., 2002). The use of artificial septum targeting and mutagenesis experiments has allowed a model to be constructed that suggests that the DivIB/DivIC/FtsL trimeric complex may play a direct or indirect role in peptidoglycan metabolism at the septum through interactions with PBP2B (Rowland *et al*., 2010).

Interestingly, no DivIB orthologue is found in bacteria lacking cell walls, implying a role in peptidoglycan synthesis or remodelling (Margolin, 2000). Further evidence to support this has previously been reported; the inability of a *B. subtilis divIB* null mutant to sporulate results in a thickening of the polar septa, akin to mutants deficient in sporulation-specific cell wall hydrolases (Thompson *et al*., 2006). Additionally, coordinate expression of *divIB* and *murB* from the highly conserved *dcw* (division and cell wall) cluster, containing many genes involved in peptidoglycan biosynthesis and cell division, is necessary for growth and sporulation in *B. subtilis* (Real and Henriques, 2006). Finally, an *S. pneumoniae ΔdivIB* mutant shows increased sensitivity to β-lactam antibiotics, whose primary target is the transpeptidase domain of PBPs (Le Gouellec *et al*., 2008).

DivIB consists of an N-terminal cytoplasmic segment, a single membrane-spanning region and an extracytoplasmic domain. The extracytoplasmic region of DivIB is comprised of three subdomains, α, β and γ (Fig. 1A), as determined by nuclear magnetic resonance spectroscopy of *Geobacillus stearothermophilus* DivIB, small-angle X-ray scattering of *S. pneumoniae* DivIB, and X-ray crystallography of *E. coli* and *Yersinia pestis* FtsQ (Robson and King, 2006; van den Ent *et al*., 2008; Masson *et al*., 2009). The α domain shows homology to the POTRA (polypeptide transport-associated) domain, which is thought to act as a molecular chaperone in both prokaryotes and eukaryotes (Sanchez-Pulido *et al*., 2003). The β domain was shown to contain a rare left-handed connection between parallel β-sheets by NMR spectroscopy (Robson and King, 2006). The γ domain is unstructured and highly variable in length, ranging from ~ 20 residues (e.g. *B. subtilis*) to over 60 residues (e.g. *S. pneumoniae* and *S. aureus*) and is absent from some species (e.g. *Haemophilus influenzae* and *Legionella pneumophila*).

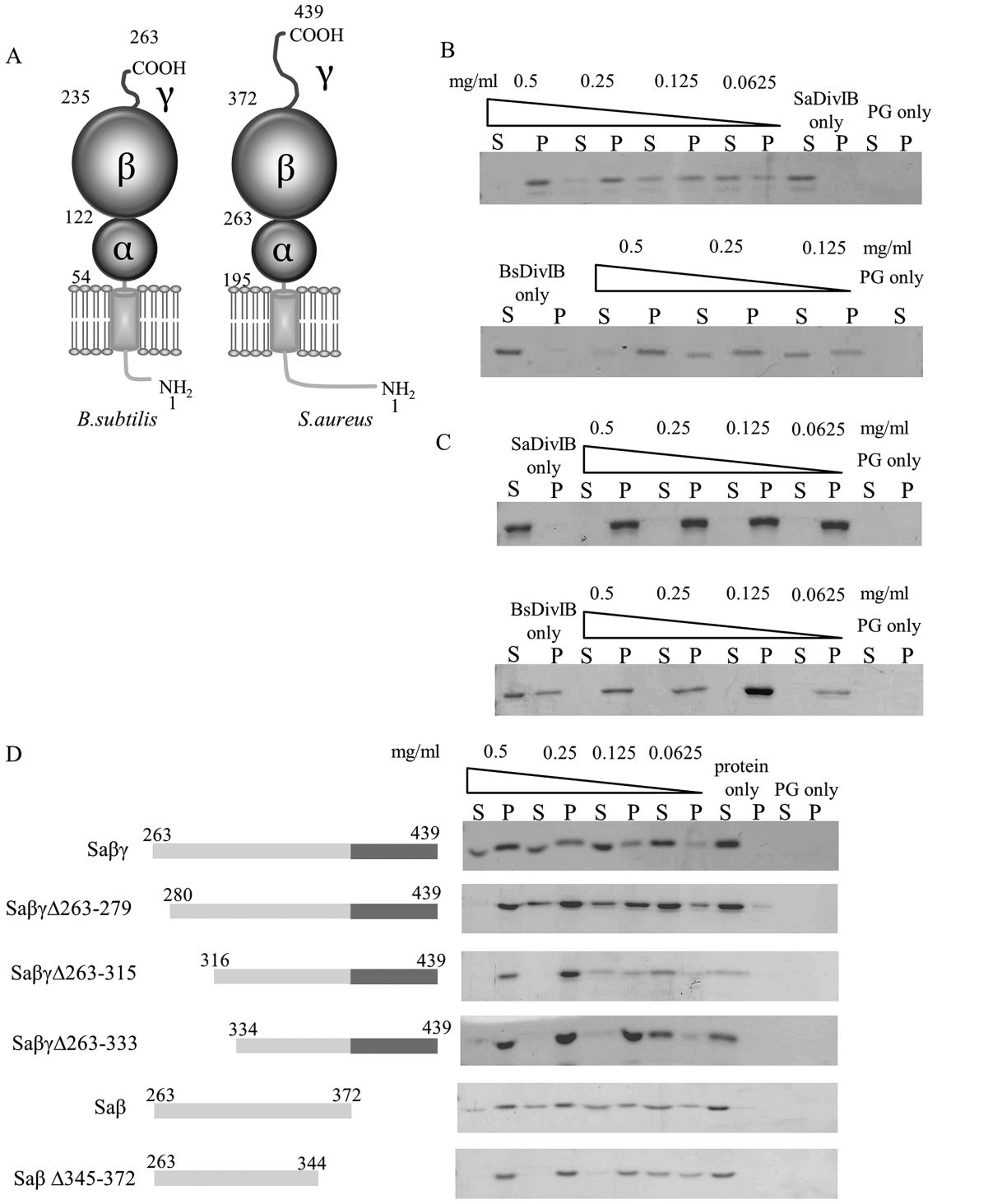

Fig. 1. DivIB is a peptidoglycan-binding protein.
A. Schematic representation of the domain architecture of *B. subtilis* and *S. aureus* DivIB. The extracytoplasmic region is separated into three domains, α, β and γ. The numbers correspond to the amino acids at the domain boundaries based on structural alignments with *G. stearothermophilus* DivIB.
B and C. Sedimentation analysis of SaDivIB and BsDivIB, corresponding to the α, β and γ subdomains, binding to *S. aureus* (B) and *B. subtilis* (C) purified peptidoglycan. Recombinant protein was incubated with increasing concentrations of purified peptidoglycan for 2 h at 37°C. Samples were then separated into supernatant (S) and pellet (P) fractions prior to separation using SDS-PAGE.
D. Sedimentation analysis of truncated SaDivIB proteins binding to *S. aureus* purified peptidoglycan. Schematics of the truncations with corresponding amino acid residues are shown on the left, while Coomassie-stained gels of the separated supernatant (S) and pellet (P) fractions are shown on the right.

Our previous work has revealed that DivIB forms part of the division complex (Steele *et al.*, 2011); however, its role in cell division, and specifically in peptidoglycan metabolism, is still currently unknown. In this study we have shown that *B. subtilis* and *S. aureus* DivIB bind directly to peptidoglycan and represent a novel class of peptidoglycan-binding protein. Furthermore, the binding domain of *S. aureus* DivIB has been mapped. We have used conditional mutation analysis to show that DivIB is required for division of *S. aureus*, being necessary for septal completion, but not initiation. This provides a tool to determine the morphological checkpoints during septation.

Results

The extracellular domain of DivIB is a novel peptidoglycan-binding protein

DivIB is a bitopic membrane protein composed of an N-terminal cytoplasmic domain, a membrane-spanning domain and a C-terminal extracytoplasmic region. Domain swapping experiments in *E. coli* and *B. subtilis* have shown that the extracytoplasmic domain of FtsQ and DivIB is topologically separate and sufficient for cell division (Guzman *et al.*, 1997; Katis and Wake, 1999). To investigate putative DivIB biochemical function, the extracytoplasmic domain of DivIB from *B. subtilis* (BsDivIB; residues 54–263) and *S. aureus* (SaDivIB; residues 195–439) were produced as his-tagged recombinant proteins (Supplementary Fig. S1A) and tested for the ability to bind purified peptidoglycan using a sedimentation assay (see *Experimental procedures*). SaDivIB efficiently bound purified native peptidoglycan in a substrate-concentration-dependent manner (Fig. 1B). Binding of BsDivIB to native peptidoglycan was also observed, although precipitation of the recombinant protein was observed under the conditions used (Fig. 1C). Furthermore, both BsDivIB and SaDivIB bound to non-native peptidoglycan, indicating that the binding ability of DivIB is not affected by the composition of the peptide stem, which contains meso-diamoinopimelic acid at residue 3 in *B. subtilis* or L-Lysine, to which a pentaglycine cross bridge binds, in *S. aureus* (Fig. 1B and C). Indeed, it was observed that SaDivIB showed stronger affinity for non-native peptidoglycan compared to native peptidoglycan. This may be due to the availability of binding sites due to lower cross-linking of stem peptides in *B. subtilis* peptidoglycan. Affinity for peptidoglycan was not due to non-specific interactions since binding was not observed for cytochrome C, which has a comparable isoelectric point to SaDivIB (9.5 and 9.34 respectively) or BSA (Supplementary Fig. S1B).

To further determine the domain(s) involved in peptidoglycan affinity, truncations of SaDivIB were tested for the ability to bind peptidoglycan (Fig. 1D). Truncations were made based on alignments with the domain architecture for *G. stearothermophilus* DivIB to attempt to reduce protein misfolding and produced as his-tagged recombinant proteins (Supplementary Fig. S1A). Sedimentation assays revealed that both the α and γ domains are dispensable for peptidoglycan binding of *S. aureus* DivIB. Progressive removal of the N-terminus of the β domain did not abolish affinity for peptidoglycan, inferring that the binding site of SaDivIB lies within the C-terminus of the β domain (residues 333–372). Additionally, removal of the extreme C-terminus of the β domain did not affect the binding of SaDivIB, further mapping the peptidoglycan binding site to residues 334–344 of the β domain. However, all truncations tested in this study showed some degree of affinity for peptidoglycan, and so it cannot be ruled out that another binding site is present, but not essential, for binding under the conditions used in this study. Since the assay used to perform these experiments is qualitative, conclusions could not be drawn about the affinity of DivIB binding to peptidoglycan. Thus, a semi-quantitative method was used to investigate this further.

To investigate peptidoglycan binding semi-quantitatively, SaDivIB was conjugated to the fluorescent dye Cy2 and the peptidoglycan binding kinetics were examined (see *Experimental procedures*). It was found that a significant amount of non-specific peptidoglycan binding of Cy2-BSA occurred without addition of 0.05% (v/v) Tween 20, and so was subsequently included in the binding buffer in all experiments (Supplementary Fig. S1C, Li and Howard, 2010). SaDivIB bound to purified *S. aureus* peptidoglycan in a concentration-dependent and saturable manner. This binding was dependent on pH, with highest affinity observed at pH5 and greatly reduced binding at higher pH (Fig. 2A).

To determine if increased affinity for peptidoglycan at lower pH correlates with physiologically relevant conditions, protonation of *S. aureus* cell walls was investigated by measurement of the total amount of cell wall-bound fluorescence using FITC, a pH-sensitive dye with an optimal pH range of 7–9 (Calamita *et al.*, 2001). Unprotonated bacterial cell walls result in available linkage sites for FITC, while cell walls possessing a lower pH greatly reduces the concentration of aliphatic amines which results in lower FITC binding. Here, similar results for FITC conjugation to cell walls were observed for *S. aureus* to that previously reported for *B. subtilis* (Calamita *et al.*, 2001). Cell walls were more readily labelled at pH 8 after dissipation of the proton motive force (pmf), using DCCD, resulting in loss of the low pH cell wall and an equilibrium of pH of the cell wall and surrounding environment: de-energised cells show an increase in FITC binding because of unprotonation of the cell walls by pmf disruption (Supplementary Fig. S2A and B). Hence, optimal binding of Cy2-SaDivIB to

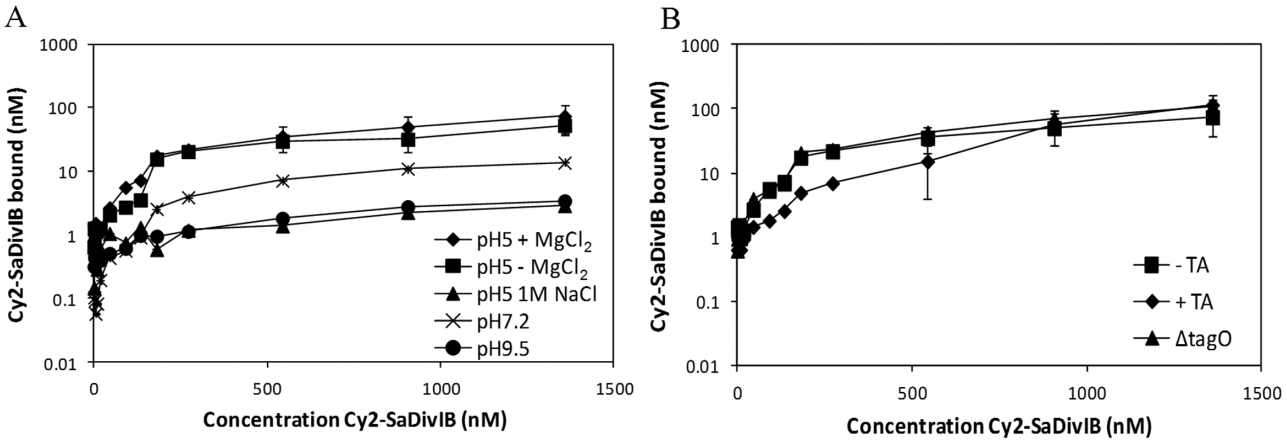

Fig. 2. SaDivIB peptidoglycan binding.
A. The effect of conditions on Cy-SaDivIB peptidoglycan binding kinetics. Varying concentrations of Cy2-labelled SaDivIB were incubated with *S. aureus* purified peptidoglycan using binding buffer at pH 5 + $MgCl_2$ (◆), pH 5 (■), pH5 + 1 M NaCl (▲), pH 7.2 (X) and pH9.5 (●).
B. Cy2-SaDivIB binding to *S. aureus* purified peptidoglycan in the absence (■) or presence (◆) of teichoic acids (TA), and to purified *S. aureus* Δ*tagO* cell walls (▲).
All binding is displayed as three independent measurements of the concentration of bound Cy2-SaDivIB. Error bars represent the standard deviation ≥ 10 nM.

peptidoglycan at pH 5 is likely to reflect the physiological conditions of the native protein.

Peptidoglycan binding of DivIB was abolished by the addition of 1 M NaCl, indicating ionic interactions between DivIB and substrate. Addition of Mg^{2+} cations did not affect DivIB affinity for peptidoglycan. It was found however that a higher amount of Cy2-SaDivIB was dissociated from peptidoglycan during the wash stages in the absence of magnesium cations compared to the presence of cations (4 ± 0.2% lost compared to 1 ± 0.1% at the highest Cy2-SaDivIB concentration tested), suggesting that magnesium cations may act to stabilise the interaction between DivIB and peptidoglycan.

The presence of teichoic acids was found to reduce the affinity of a known peptidoglycan-binding protein (Utsui and Yokota, 1985) (*S. aureus* Cy2-PBP1) for peptidoglycan (data not shown). To investigate if the same was true for Cy2-SaDivIB, binding kinetics were analysed using either SDS- and pronase-treated broken *S. aureus* cell walls (peptidoglycan plus teichoic acids), or purified *S. aureus* peptidoglycan that had been chemically stripped of teichoic acids (Fig. 2B). An apparent K_d of 550 ± 56 nM could be calculated, representing the concentration of Cy2-SaDivIB giving half-maximum binding, for binding to cell walls (peptidoglycan plus teichoic acids). A K_d of 134 ± 9 nM was observed for binding to peptidoglycan stripped of teichoic acids, indicating higher affinity for the peptidoglycan backbone. To confirm that differences in binding affinity was due to teichoic acids and not caused by chemical modification of cell walls during the purification process, purified *S. aureus* Δ*tagO* peptidoglycan, which is devoid of teichoic acids due to deletion of the enzyme responsible for the first step in of wall teichoic acid synthesis, was used as substrate. An apparent K_d of 221 ± 81 nM was calculated, indicating that the presence of teichoic acids decreases the affinity of DivIB for peptidoglycan, presumably due to masking of available binding sites.

S. aureus *DivIB localises transiently at midcell*

Immunoblot analysis of native *B. subtilis* DivIB showed the protein to be associated with the cytoplasmic membrane, and also the cell wall *in vivo* (Harry *et al.*, 1993). The ability of *S. aureus* DivIB to bind to cell wall *in vivo* was therefore determined using α-DivIB antiserum. *S. aureus* DivIB associated with both cytoplasmic membrane and cell wall fractions (Fig. 3A). It is unlikely that detection of DivIB in the cell wall fraction was due solely to contamination with unfractionated cells and/or membranes, as immunoblot analysis using antiserum against *S. aureus* YneS, a known membrane-bound protein (J. Garcia-Lara, unpublished) showed only minimal detection in the cell wall fraction.

Bacterial two-hybrid analysis has previously indicated that DivIB is a component of the *S. aureus* divisome (Steele *et al.*, 2011). Initial attempts to determine the subcellular localisation of DivIB utilised a C-terminal GFP fusion protein (ALB2; SH1000 *divIB-gfp* pGL485). Unexpectedly, no obvious midcell localisation of DivIB-GFP was observed. Instead, two or three discrete peripheral foci on each cell, or each hemisphere of dividing cells, were detected (Fig. 3B). A line of fluorescence was also sometimes observed that connected two of the peripheral foci. It may be that this localisation pattern is due to the degradation of GFP due to fusion to the C-terminus of DivIB and

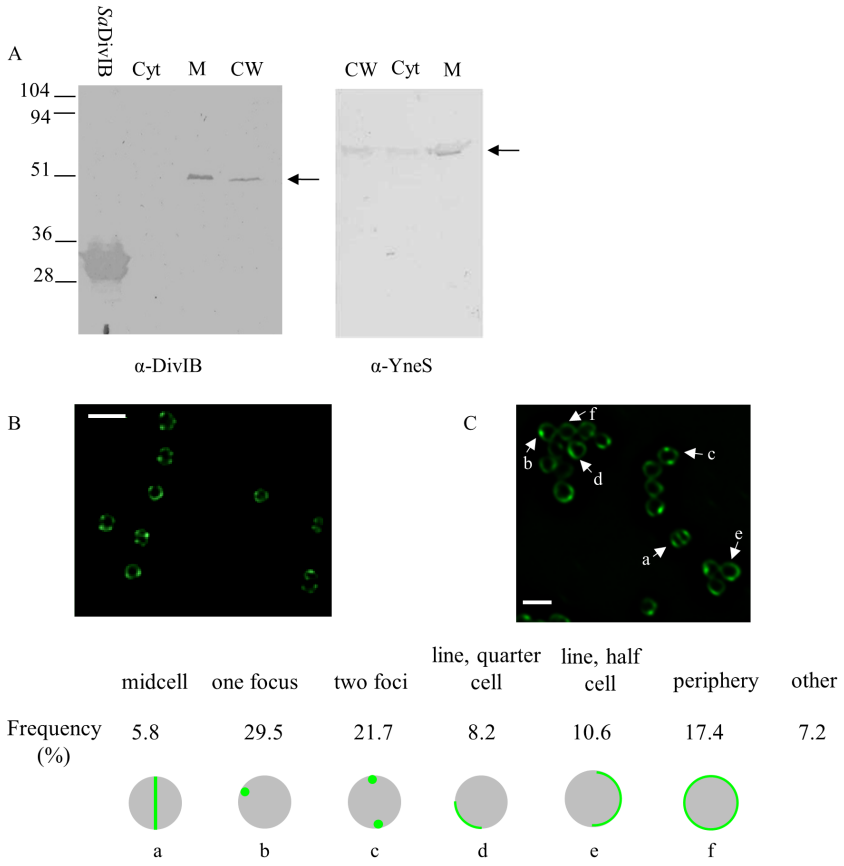

Fig. 3. Localisation of DivIB in *S. aureus*.
A. Subcelluar localisation of DivIB in ALB1 (SH1000 *atl::ery spa::kan*). Equal amounts of cellular material corresponding to the cytoplasmic (Cyt), membrane (M) or cell wall (CW) fraction were loaded. As a control, fractions were probed with rabbit α-YneS. Arrows indicate the position of detected protein.
B. Localisation of DivIB-GFP in ALB2 (SH1000 *divIB-gfp* pGL485). Scale bar = 1 μm.
C. Localisation of YFP-DivIB in ALB26-yfp (SH1000 Δ*divIB geh::P*$_{Spac}$ *eYFP-divIB*). The frequencies of different localisation patterns are shown ($n = 207$) with a representative cell for each localisation.

thus export outside the cytoplasm. However, immunofluorescence microscopy with α-DivIB antibodies showed a similar localisation pattern at that seen for DivIB-GFP (data not shown).

To fully confirm localisation of *S. aureus* DivIB, and to exclude any potential polar effects on downstream genes due to expression of the fusion proteins, an N-terminal YFP fusion protein was constructed. Strain ALB26-yfp (SH1000 *geh::P*$_{Spac}$*-yfp-divIB ΔdivIB*) expresses a single copy of *yfp-divIB* under the control of P$_{Spac}$ ectopically inserted at lipase based on the pCL84 integrase system (Lee *et al*., 1991). YFP-DivIB was found to localise in a range of different patterns, including two foci or line of fluorescence at the presumptive midcell, as single focus at the cell membrane, or as uniform fluorescence throughout the membrane of the cell (Fig. 3C). These results confirm the localisation patterns observed using DivIB-GFP and immunolocalisation, suggesting that DivIB localisation at midcell in *S. aureus* may only be transient.

DivIB is essential for S. aureus *growth*

Staphylococcus aureus divIB, SAOUHSC_01148, was identified to be putatively essential by a high-density transposon screen for genes important for cell viability (Chaudhuri *et al*., 2009). Bioinformatic analysis of the *S. aureus divIB* chromosomal regions indicated that the gene is part of the *dcw* cluster and is located directly upstream of *ftsA* and *ftsZ* (Fig. 4A). Initial attempts to confirm essentiality of *divIB* involved construction of a *S. aureus* conditional mutation. However, due to the complexity of transcription of the *dcw* cluster and likely polar effects on downstream *ftsAZ*, the role of *divIB* could not be established using this method (data not shown).

To overcome this, and to determine the role of *divIB*, a conditional mutant was constructed where a full-length copy of *divIB* under the control of P$_{Spac}$ was inserted ectopically at the *geh* locus, allowing an in-frame deletion of the gene from its native chromosomal location without disruption of expression of downstream genes (Fig. 4B). To ensure minimal expression from P$_{Spac}$ in the absence of inducer, *lacI* was constitutively overexpressed from a multicopy plasmid, pGL485 (Cooper *et al*., 2009), resulting in strain ALB27 (*geh::P*$_{Spac}$*-divIB ΔdivIB* pGL485). ALB27 did not grow in the absence of inducer (IPTG), whereas in the presence of IPTG ALB27 had a growth rate comparable to wild-type strain VF17 (SH1000 pGL485) both on solid and in liquid media (Fig. 4C). ALB27 (*geh::P*$_{Spac}$*-divIB ΔdivIB* pGL485) was also unable to grow on agar plates in the

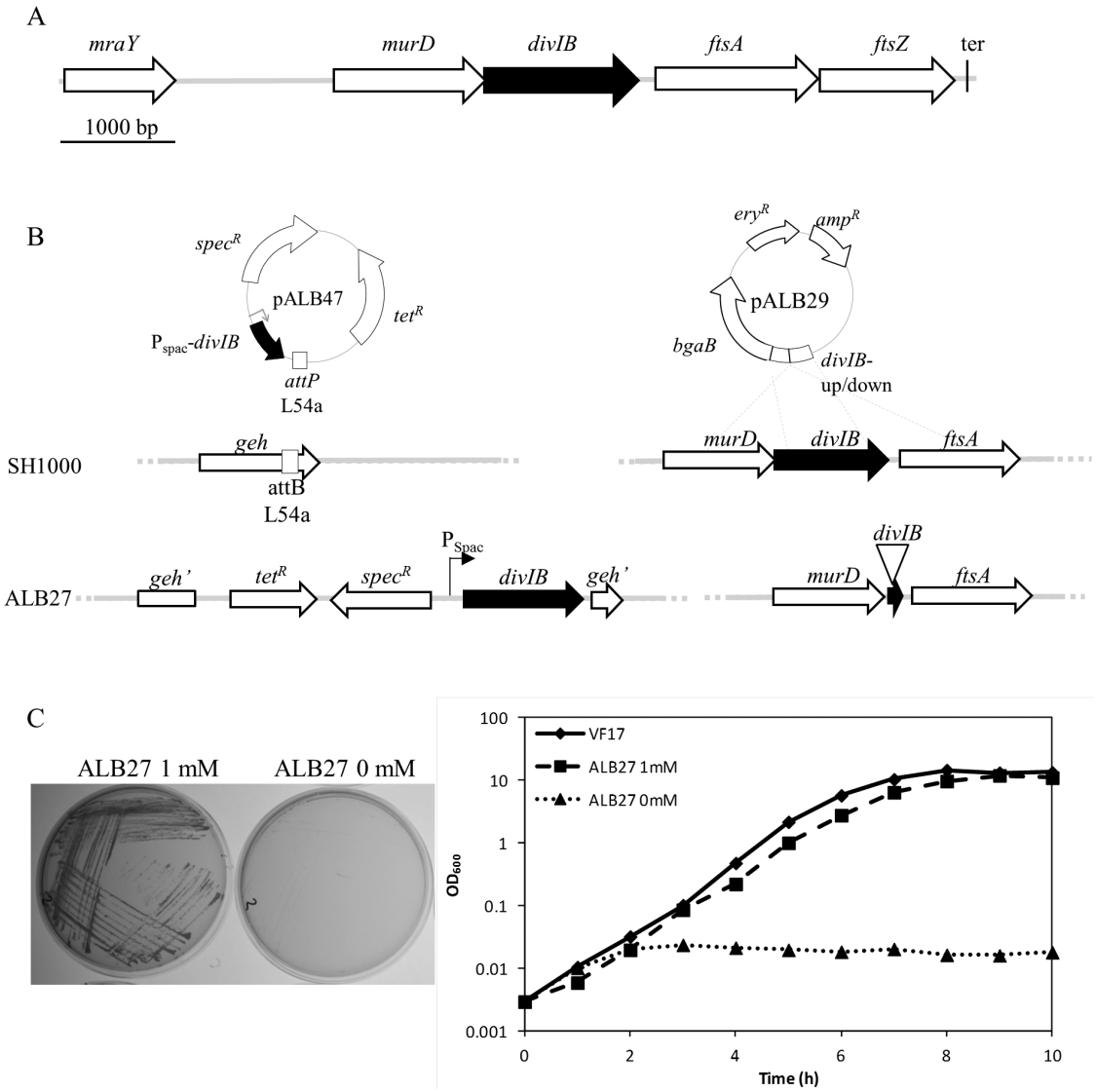

Fig. 4. Construction and verification of a conditional lethal *divIB* mutation.
A. Schematic of chromosomal location of *S. aureus divIB*. A putative transcription terminator (ter) after *ftsZ* is highlighted.
B. Representation of the ALB26 (*geh::P*$_{Spac}$*-divIB ΔdivIB*) chromosomal construct. Integration of pALB47 at *S. aureus* lipase (*geh*) resulted in an ectopic copy of *divIB* under the control of P$_{Spac}$. Resolution of a double-crossover event of pALB29 could then be achieved to allow in-frame deletion of *divIB* from its native chromosomal location.
C. DivIB is required for the growth of *S. aureus*. Growth of ALB27 (*geh::P*$_{Spac}$*-divIB ΔdivIB* pGL485) on BHI plates in the presence (1 mM) or absence (0 mM) of IPTG is shown on the left. The right hand panel shows growth of strains VF17 (SH1000 pGL485; ◆) and ALB27 (*geh::P*$_{Spac}$*-divIB ΔdivIB* pGL485) in the presence (■) or absence (▲) of 1 mM IPTG as detected by OD$_{600}$. Strain VF17 (SH1000 pGL485) was unaffected by addition by IPTG and so only growth in the absence of inducer is shown.

absence of IPTG when incubated at 30°C (data not shown). Therefore, *divIB* is essential for growth of *S. aureus*.

Depletion of DivIB results in increased cell size

To investigate the effect of DivIB depletion on cellular morphology, ALB27 (*geh::P*$_{Spac}$*-divIB ΔdivIB* pGL485) was examined following growth in the absence or presence of the inducer IPTG. In the presence of inducer, cells showed a similar morphology to wild-type cells (Fig. 5A). However, after 2 h incubation in the absence of inducer, ALB27 cells showed an increased cell size. It is important to note that this morphology differs to that previously observed for *S. aureus* depleted of FtsZ (Pinho and Errington, 2003) or EzrA (Steele *et al.*, 2011), which results in very large spherical single cells. DivIB-depleted *S. aureus* cells showed a range of phenotypes, including misplacement of septa resulting in 'hamburger' cells due to initiation of new rounds of septum formation in parallel planes without the

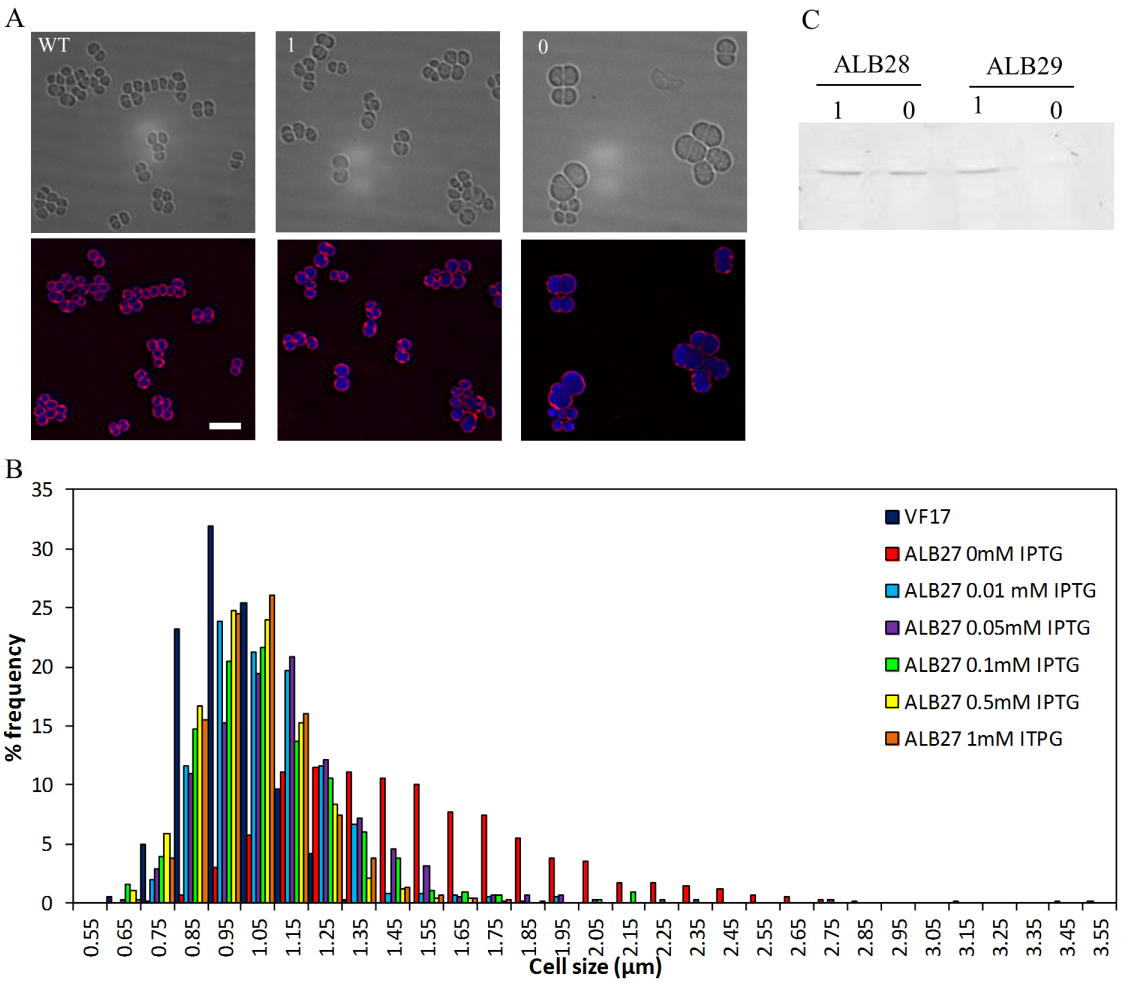

Fig. 5. Role of DivIB in cell division.
A. Microscopic analysis of the phenotype of ALB27 (*geh::P*$_{Spac}$*-divIB ΔdivIB* pGL485). Top panels show phase-contrast images of VF17 (WT; SH1000 pGL485) and ALB27 after 120 min growth in the presence (1) or absence (0) of 1 mM IPTG, while bottom panels show cell membrane staining with FM4-64 (red) and DNA staining with DAPI (blue). Scale bar = 4 μm.
B. Frequency of cell diameter of ALB27 (*geh::P*$_{Spac}$*-divIB ΔdivIB* pGL485) grown in different inducer concentrations. VF17 (SH1000 pGL485) and ALB27 were grown for 120 min in the presence of 0–1 mM IPTG. VF17 cell diameter was unaffected by addition of IPTG and therefore only measurements for 0 mM IPTG is shown. Diameter was measured across the longest axis of the cell.
C. Levels of DivIB in ALB28 (*spa::kan* pGL485) and ALB29 (*spa::kan geh::P*$_{Spac}$*-divIB ΔdivIB* pGL485) following 120 min growth in the presence (1) or absence (0) of 1 mM IPTG were detected by Western blot of total protein extract using α-DivIB. An equal number of cells, as determined by OD_{600}, were loaded.

completion of previous rounds of septation, bulging of the cell wall and eventual lysis (Fig. 5A). Measurement of cells found that in the presence of 1 mM IPTG, the mean cell diameter of ALB27 was similar to wild-type VF17 cells (mean diameter = 1 ± 0.2 μm, n = 768 and 0.9 ± 0.1 μm, n = 363 respectively). In the absence of inducer, cells showed an increased cell size (mean diameter = 1.5 ± 0.4 μm, n = 980). A small proportion of ALB27 cells showed an increased cell size (> 1.25 μm) even at 1 mM IPTG, indicating that expression of DivIB from the Spac promoter doesn't fully restore cellular morphology. However, this phenotypic change was most notable in the absence of inducer, with a high proportion of very large cells up to 3.5 μm in diameter seen (Fig. 5B). Western blot analysis shows undetectable levels of DivIB after growth in the absence of inducer (Fig. 5C), indicating the observed morphology is due to depletion of DivIB.

DivIB is required for completion, but not initiation, of septum formation

Previous work has shown that *S. aureus* synthesises cell wall specifically at the septum, and that nascent cell wall synthesis is dispersed or does not occur in the absence of early components of the divisome (Pinho and Errington, 2003; Steele *et al.*, 2011). To investigate if DivIB plays a

role in the synthesis of cell wall, a fluorescent derivative of vancomycin (Van-Fl) was used to label nascent peptidoglycan in DivIB-depleted cells. Almost all wild-type *S. aureus* cells (VF17; SH1000 pGL485) and ALB27 (*geh::*P_{Spac}*-divIB ΔdivIB* pGL485) grown in the absence or presence of IPTG showed septal peptidoglycan synthesis (Fig. 6A). However, different staining morphologies were observed for VF17 and ALB27 grown in the presence of inducer compared to ALB27 cells grown in the absence of IPTG. Forty-eight per cent of VF17 cells and 43% of ALB27 cells grown in the presence of IPTG showed either a ring or line of fluorescence at midcell, and 23% and 22%, respectively, showed an 'x' or 'y' staining pattern, characteristic of separating newly formed daughter cells (Fig. 6B, Turner *et al*., 2010). A large proportion (75%) of ALB27 cells grown in the absence of inducer also showed a midcell staining pattern. In addition, 13% of DivIB-depleted cells showed multiple or aberrant fluorescent rings. These unusual staining patterns were observed exclusively in cells > 1.25 μm, indicating misplacement of the cell wall biosynthesis machinery. Further analysis of midcell staining found that 72% and 52% of VF17 and induced ALB27 cells showed a ring of fluorescence at the division site which corresponds to a ring of new peptidoglycan, and 28% and 33% (VF17 and ALB27 respectively) showed a fluorescent line across the cell, corresponding to a plate of nascent peptidoglycan that is the completed septum (Fig. 6C). In the absence of IPTG, ALB27 cells showed a ring of fluorescence that appeared to be equivalent to the cell diameter. Only a small proportion of DivIB-depleted cells appeared to form complete septa (12%), presumably due to residual DivIB present from prior to DivIB-depletion. Growth of *S. aureus* has been proposed to occur in between cell division events via specific hydrolysis of existing cell wall material (Turner *et al*., 2010). A distinct ring of nascent peptidoglycan between two cells was also often observed, indicating that cells are undergoing hydrolytic growth of the cell wall in the absence of the formation of complete septa. Thus, in the absence of DivIB, initiation of septum formation is not affected, resulting in the synthesis of a large 'band' (piecrust) of nascent peptidoglycan at midcell. However the ensuing formation of the septal plate is blocked.

Scanning electron microscopy of ALB27 (*geh::*P_{Spac}*-divIB ΔdivIB* pGL485) grown in the absence of IPTG revealed a band of cell wall at midcell which was not detectable in wild-type cells (VF17) or ALB27 cells grown in the presence of IPTG (Fig. 7A), and may represent the piecrust. This is likely due to the continued hydrolytic growth and turnover of the existing cell wall of DivIB-depleted cells in the absence of new septum formation, revealing cell wall architecture not observed in wild-type cells. Transmission electron microscopy of DivIB-depleted cells also confirmed the misplacement of septa, resulting in more than one initiation site within dividing cells, bulging of the cell wall and cell lysis (Fig. 7B).

To investigate the architecture of the cell wall in the absence of DivIB in more detail, atomic force microscopy (AFM) of purified sacculi of ALB27 (*geh::*P_{Spac}*-divIB ΔdivIB* pGL485) cells grown in the absence of inducer was performed. Thick bands of peptidoglycan were observed, confirming the formation of piecrusts in cells depleted of DivIB (Fig. 7C). Incomplete septa were also occasionally seen, and may represent cells that were at different stages of the cell cycle when cell division was blocked by depletion of DivIB. Thus, investigation of the macromolecular architecture of the cell wall in the absence of DivIB confirms the results observed for fluorescence microscopy, resulting in the initiation of septation and the formation of the piecrust. However, completion of septum formation is severely affected in the absence of DivIB.

Localisation of cell division proteins in the absence of DivIB

The significant increase in cell size and misplacement of septa in *S. aureus* cells depleted of DivIB suggests that recruitment of the divisome to the midcell may be altered in the absence of this protein. The effect of DivIB depletion on the ability of divisome components to localise to midcell was therefore investigated.

In *B. subtilis*, EzrA localises to the midcell in an FtsZ-dependent manner where it is thought to be a negative regulator of Z ring formation (Levin *et al*., 1999). Time-lapse microscopy has shown that EzrA localises concomitantly with FtsZ, with a time delay of at least 20% of the cell cycle before late proteins, including DivIB, assemble at midcell (Gamba *et al*., 2009). Previous analysis of the role of EzrA in *S. aureus* has shown that the protein likely acts as a scaffold for the assembly of the divisome (Jorge *et al*., 2011; Steele *et al*., 2011). It was therefore investigated if depletion of DivIB, a late division protein, affected the localisation of the early protein EzrA in *S. aureus*. Localisation of EzrA in VF104 (*ezrA-GFP+* pGL485) and ALB30 (*ezrA-GFP+ geh::*P_{Spac}*-divIB ΔdivIB* pGL485) was determined using a C-terminal GFP+ fusion. Fluorescence was detected as a ring or line at the septum in almost all VF104 cells and ALB30 grown in the presence of IPTG (Fig. 8A). Midcell localisation of EzrA-GFP+ was also observed for the majority of ALB30 cells grown in the absence of IPTG with a cell diameter < 1.25 μm (Fig. 8B). However, for ALB30 cells with a diameter > 1.25 μm, a striking localisation pattern was observed, with fluorescence almost exclusively observed as multiple or aberrantly formed rings. Interestingly, EzrA-GFP+ ring size appeared to be equivalent to the cell diameter for large DivIB-depleted cells. Furthermore, the localisation pattern

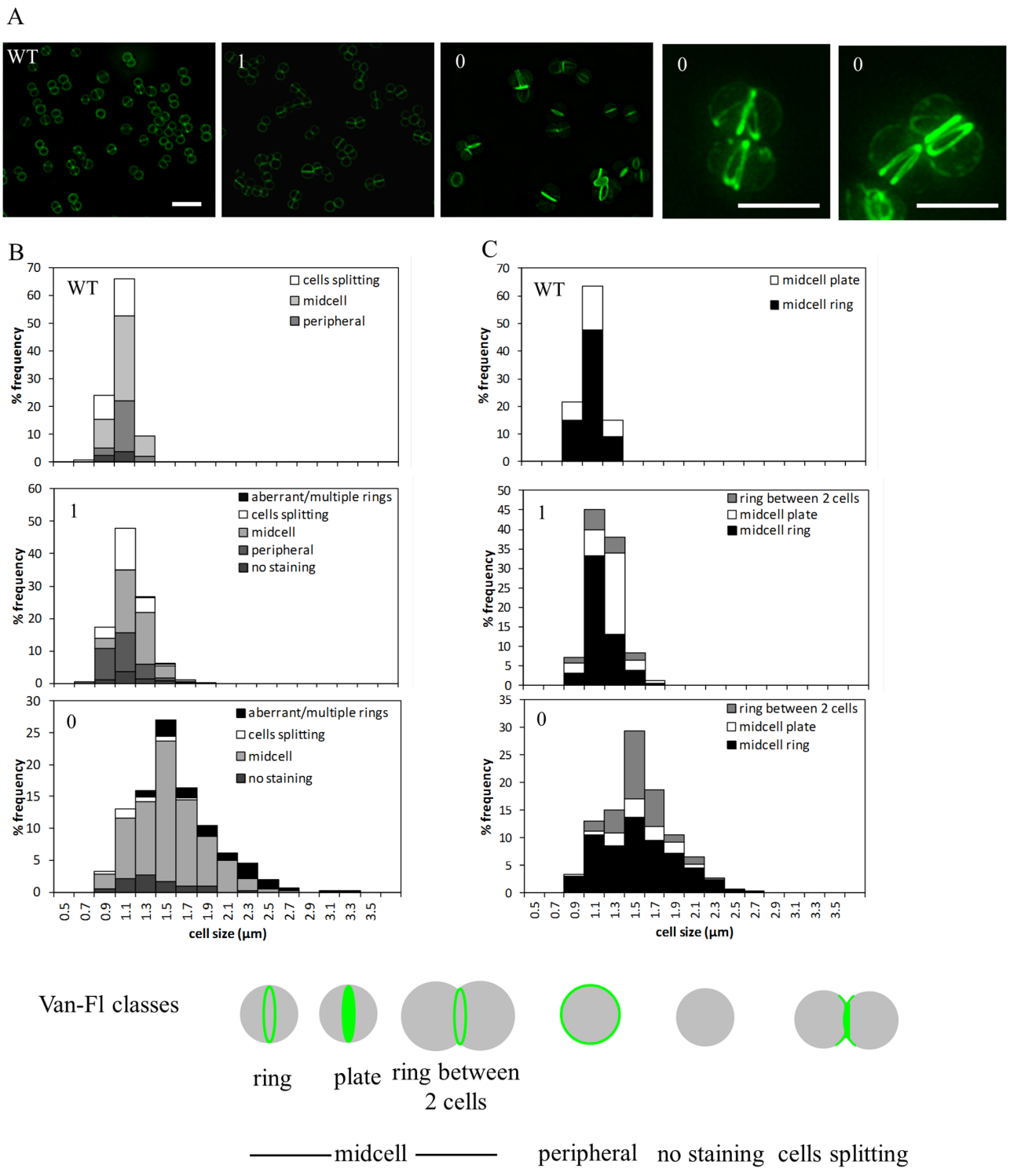

Fig. 6. Role of DivIB in peptidoglycan biosynthesis.
A. Van-Fl labelling of nascent cell wall synthesis in VF17 (WT; SH1000 pGL485) and ALB27 (*geh::P*$_{Spac}$*-divIB ΔdivIB* pGL485) grown for 120 in the presence (1) or absence (0) of 1 mM IPTG. Scale bar = 4 µm.
B. Frequency of Van-Fl staining cellular phenotypes of VF17 (WT; SH1000 pGL485) and ALB27 (*geh::P*$_{Spac}$*-divIB ΔdivIB* pGL485) grown for 120 in the presence (1) or absence (0) of 1 mM IPTG. Cells were given one of five Van-Fl staining phenotypes in relation to cell diameter. The number of cells measured was 278, 362 and 421 respectively.
C. Frequency of midcell Van-Fl staining cellular phenotypes of VF17 (WT; SH1000 pGL485) and ALB27 (*geh::P*$_{Spac}$*-divIB ΔdivIB* pGL485) grown for 120 in the presence (1) or absence (0) of 1 mM IPTG. Midcell Van-Fl staining phenotypes were assigned as a plate or ring of nascent peptidoglycan as determined by analysis of Z stacks of cells. The number of cells measured was 134, 153 and 306 respectively.

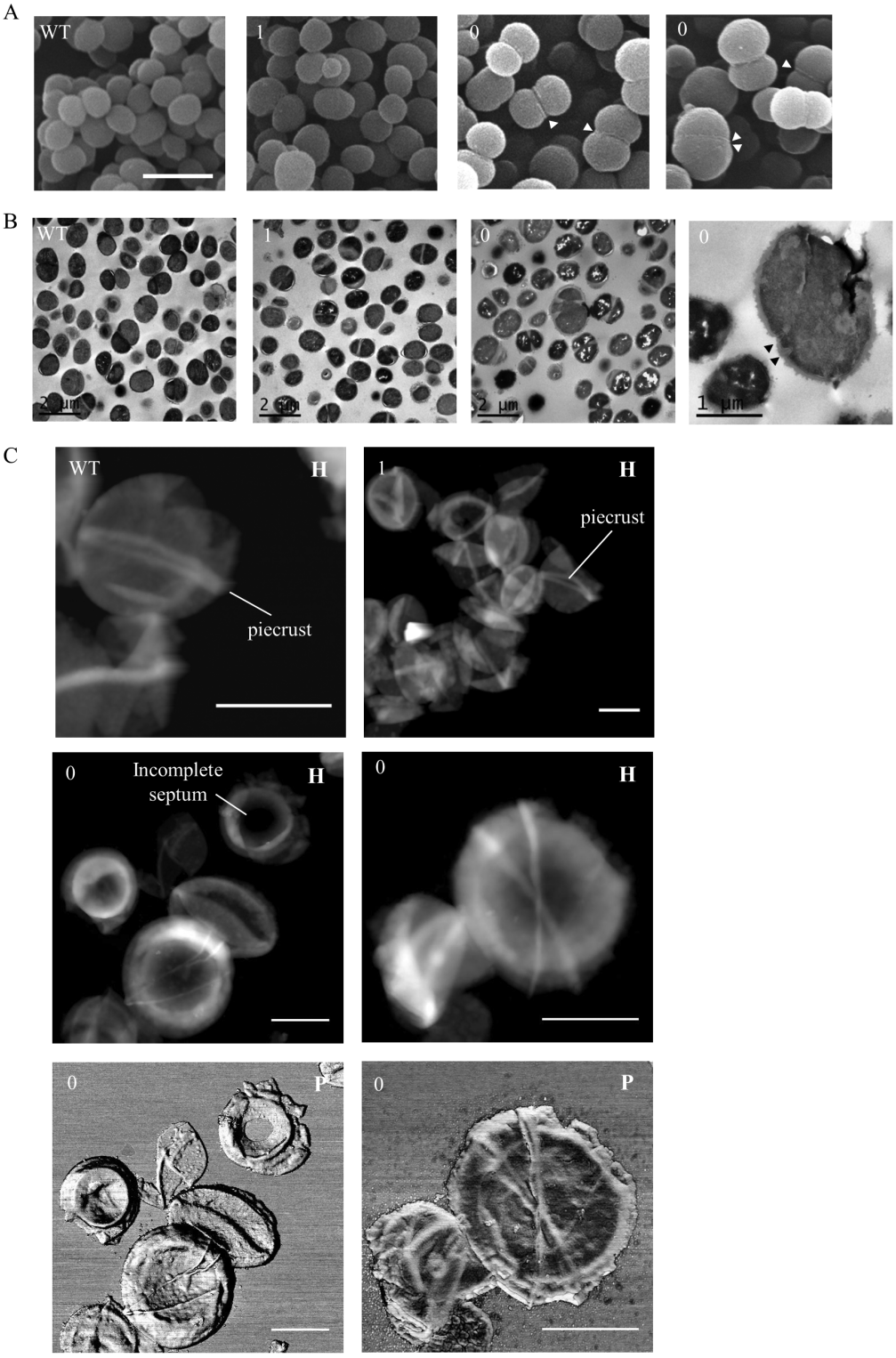

Fig. 7. Role of DivIB in cellular morphology.
A and B. Scanning (A) and transmission (B) electron micrographs of VF17 (WT, SH1000 pGL485) and ALB27 (*geh::*P_{Spac}*-divIB ΔdivIB* pGL485) grown for 120 min in the presence (1) or absence (0) of 1 mM IPTG. Scale bar in A = 2 µm. White arrowheads in A depict bands of peptidoglycan observed at midcell. Black arrowheads in B show sites aberrant sites of septum initiation.
C. AFM height (H) and phase (P) images of VF17 (WT; SH1000 pGL485) and ALB27 (*geh::*P_{Spac}*-divIB ΔdivIB* pGL485) sacculi purified from cells grown in the presence (1) and absence (0) of IPTG. Scale bar = 1 µm. Scales: WT H 150 nm; ALB27 (1) H 150 nm; ALB27 (0) left hand panel H 250 nm; right hand panel H 150 nm.

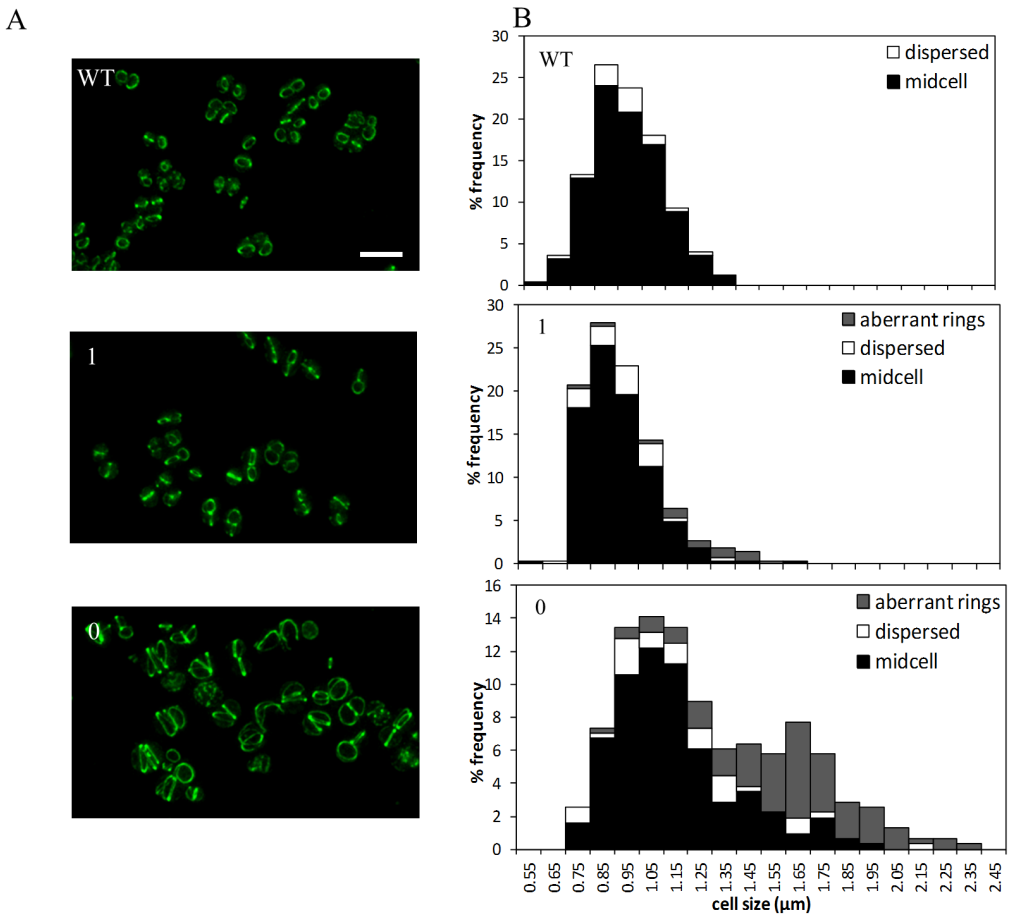

Fig. 8. Role of DivIB in localisation of the cell division machinery.
A. Localisation of EzrA-GFP+ in VF104 (WT; SH1000 *ezrA-GFP+* pGL485) and ALB30 (*ezrA-GFP+ geh::P*$_{Spac}$*-divIB ΔdivIB* pGL485) grown for 120 min in the presence (1) or absence (0) of 1 mM IPTG. Scale bar = 4 μm.
B. Frequency of EzrA-GFP+ localisation in VF104 (WT; SH1000 ezrA-GFP+ pGL485) and ALB30 (*ezrA-GFP+ geh::P*$_{Spac}$*-divIB ΔdivIB* pGL485) grown for 120 in the presence (1) or absence (0) of 1 mM IPTG. Localisation patterns were classified as midcell, dispersed or aberrant rings in relation to cell size. The number of cells measured was 249, 265 and 312 respectively.
C. Colocalisation of EzrA-GFP+ (green) and FtsZ (red) in ALB32 (SH1000 *spa::kan ezrA-GFP+* pGL485) and ALB33 (*spa::kan ezrA-GFP+ geh::P*$_{Spac}$*-divIB ΔdivIB* pGL485) grown for 120 min in the presence (1) or absence (0) of 1 mM IPTG. FtsZ was detected by immunofluorescence. Cell diameter could not be measured due to the treatment of cells with lysostaphin to allow access of antibodies to intracellular protein.
D. Localisation of GpsB-GFP+ in VF94 (WT; SH1000 *gpsB-GFP+* pGL485) and ALB31 (*gpsB-GFP+ geh::P*$_{Spac}$*-divIB ΔdivIB* pGL485) grown for 120 min in the presence (1) or absence (0) of 1 mM IPTG. Scale bar = 4 μm.
E. Frequency of GpsB-GFP+ localisation in VF94 (WT; SH1000 *gpsB-GFP+* pGL485) and ALB31 (*gpsB-GFP+ geh::P*$_{Spac}$*-divIB ΔdivIB* pGL485) grown for 120 in the presence (1) or absence (0) of 1 mM IPTG. Localisation patterns were classified as midcell, foci between recently divided cells, dispersed or aberrant rings in relation to cell size. The number of cells measured was 298, 242 and 292 respectively.
F. Colocalisation of Pbps and nascent peptidoglycan synthesis in VF17 (SH1000 pGL485) and ALB27 (*geh::P*$_{Spac}$*-divIB ΔdivIB* pGL485) grown for 120 min in the presence (1) or absence (0) of 1 mM IPTG. Pbps were stained with 1 μM bocillin 650/665 (red) and nascent peptidoglycan was stained with Van-Fl (green). Due to the weak fluorescence signal of bocillin 650/665 only single z-slices were taken. Scale bar = 4 μm.
G. Localisation of DivIC-GFP+ in AFK5 (WT; SH1000 *divIC-GFP+* pGL485) and AFK24 (*divIC-GFP+ geh::P*$_{Spac}$*-divIB ΔdivIB* pGL485) grown for 120 min in the presence (1) or absence (0) of 1 mM IPTG. Scale bar = 4 μm.

of EzrA-GFP+ suggests that EzrA is still recruited to midcell, perhaps through interactions with FtsZ.

Recruitment of all known division proteins to the midcell occurs in an FtsZ-dependent manner (Errington *et al.*, 2003). In order to determine FtsZ localisation in the absence of DivIB, and to investigate if EzrA is recruited to midcell in an FtsZ-dependent DivIB-independent manner, colocalisation of EzrA-GFP+ and FtsZ in ALB33 (*spa::kan ezrA-GFP+ geh::P*$_{Spac}$*-divIB ΔdivIB* pGL485) in the presence and absence of IPTG was performed using α-*S. aureus* FtsZ. It was found that FtsZ and EzrA-GFP+ colocalised in a ring at midcell in the control strain ALB32 (*spa::kan ezrA-GFP+* pGL485) and in ALB33 (*spa::kan ezrA-GFP+ geh::P*$_{Spac}$*-divIB ΔdivIB* pGL485) grown in the

Fig. 8. *cont.*

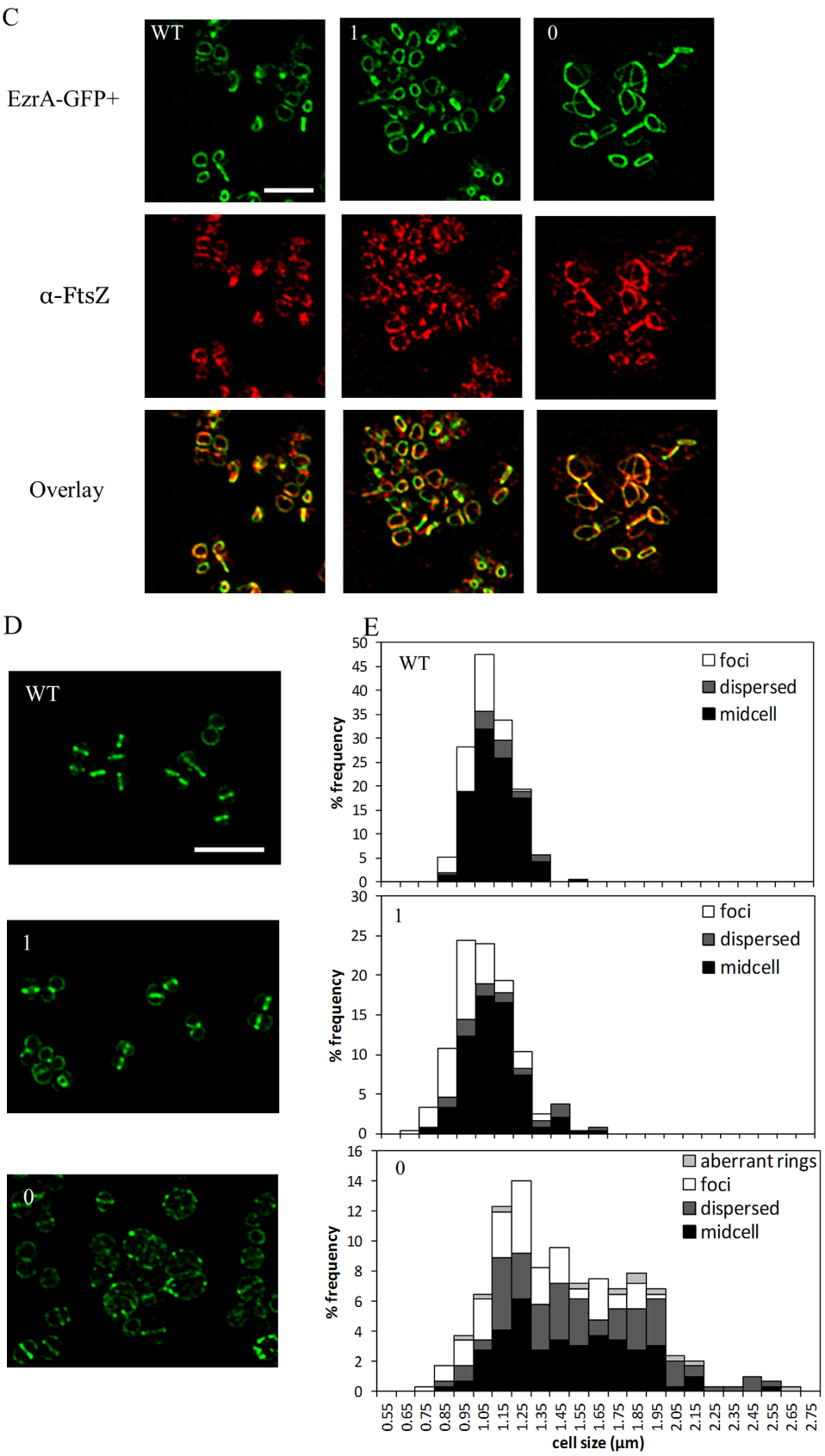

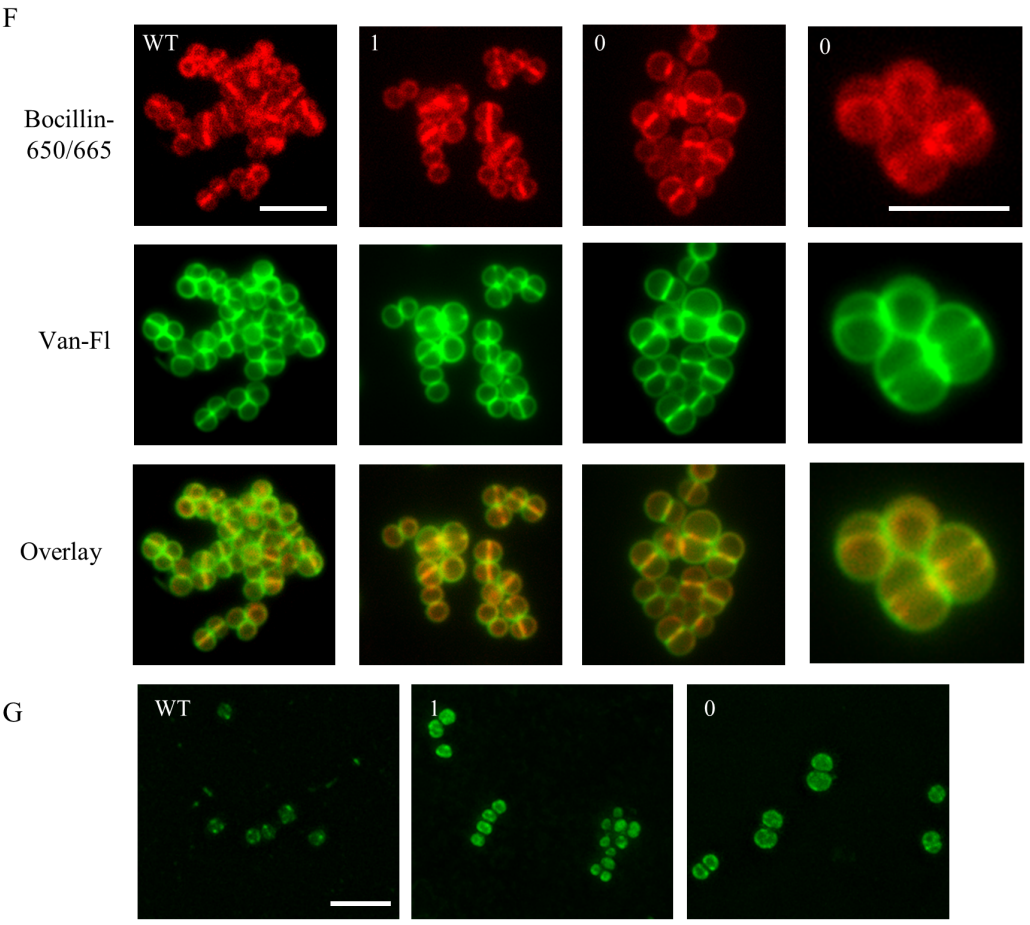

Fig. 8. *cont.*

presence of IPTG (Fig. 8C). Additionally, FtsZ immunofluorescence in ALB33 cells grown in the absence of inducer showed the formation of large, sometimes aberrant, midcell rings which coincided with EzrA-GFP+ localisation. Thus, while FtsZ can polymerise into the Z ring and recruit EzrA to midcell in the absence of DivIB, constriction of the Z ring and progression of the division cycle is blocked.

Although *ezrA* is not essential in *B. subtilis*, deletion of *ezrA* in combination with *gpsB* results in severe defects in lateral and septal peptidoglycan synthesis as a result of perturbed PBP1 localisation (Claessen *et al.*, 2008). Direct interactions have been observed between EzrA and GpsB in both *B. subtilis* and *S. aureus* (Claessen *et al.*, 2008; Steele *et al.*, 2011). It was therefore investigated if GpsB showed a similar localisation pattern to EzrA in DivIB-depleted *S. aureus* using a C-terminal GpsB-GFP+ fusion protein. GpsB-GFP+ fluorescence was observed as a line or ring in the majority of wild-type (VF94, *gpsB-GFP+* pGL485) and ALB31 (*gpsB-GFP+ geh::*P_{Spac}*-divIB ΔdivIB* pGL485) cells grown in the presence of IPTG (Fig. 8D). A bright focus of fluorescence was also often observed between two daughter cells that were undergoing separation, indicating that GpsB remains at the site of division after septum formation is complete. In ALB31 cells grown in the absence of inducer, a larger proportion of cells showed a dispersed fluorescence pattern compared to VF94 (33% compared to 8% respectively; Fig. 8E). Dispersed localisation of GpsB-GFP+ in DivIB-depleted cells was independent of cell size, indicating that, unlike EzrA, DivIB is required for localisation of GpsB at midcell.

Depletion of DivIB in *S. aureus* cells does not affect initiation of septation, but results in a cessation of completion of septum formation. To investigate if the inability to form complete septa in the absence of DivIB is due to mislocalisation of cell wall synthetic enzymes (PBPs), a fluorescent derivative of penicillin, Bocillin 650/665, was used. *S. aureus* encodes four PBPs, three of which have previously been shown to localise to midcell in wild-type cells (Pinho and Errington, 2005; Pereira *et al.*, 2007; Atilano *et al.*, 2010). Midcell localisation of the PBPs was observed for both control VF17 (SH1000 pGL485) cells and ALB27 (*geh::*P_{Spac}*-divIB ΔdivIB* pGL485) cells grown

in the presence and absence of IPTG (Fig. 8F). Staining of nascent cell wall with Van-FI revealed that the PBPs localised at the leading edge of forming septa. Furthermore, PBPs were located to aberrant rings in DivIB-depleted cells. Thus the inability of *S. aureus* cells to complete septum formation is not due to mislocalisation of cell wall synthetic enzymes, but due to depletion of DivIB.

A strong interdependency between DivIB, DivIC and FtsL has been previously established (Daniel *et al*., 1998; 2006; Ghigo *et al*., 1999; Daniel and Errington, 2000; Buddelmeijer *et al*., 2002). It is therefore possible that the inability of *S. aureus* to complete septum formation is not due directly to depletion of DivIB, but may be due to the instability of the DivIB/DivIC/FtsL complex. To investigate this, localisation of DivIC in DivIB-depleted cells was performed (Fig. 8G). However, DivIC-GFP+ fluorescence was observed as punctate foci or as a diffuse signal in wild-type cells (AFK5, *divIC-GFP+* pGL485). Fluorescence was also diffuse in AFK24 (*divIC-GFP+ geh::*P_{Spac}*-divIB ΔdivIB* pGL485) cells grown in the presence or absence of IPTG, with no defined localisation pattern observed. Thus, the role of *S. aureus* DivIC in septum completion could not be established.

Discussion

DivIB is a bitopic protein that consists of an N-terminal domain, a membrane-spanning domain and an extracytoplasmic region that is comprised of three separate domains (α, β and γ). In this study we have shown that the extracytoplasmic domain of *S. aureus* and *B. subtilis* DivIB binds peptidoglycan, and that both the α and γ domains are dispensable for this function. Although peptidoglycan hydrolase activity of DivIB has been previously suggested (Thompson *et al*., 2006), no such enzymatic activity was detected in this present study (data not shown). Domain replacement studies have shown that the extracytoplasmic domain of *B. subtilis* DivIB, or the orthologous periplasmic domain of *E. coli* FtsQ, is essential for function (Buddelmeijer *et al*., 1998; Katis and Wake, 1999; Chen *et al*., 2002), suggesting that affinity for peptidoglycan may be important for DivIB function. Although dispensable for interaction with the cell wall, the α domain is important for septal localisation (Goehring *et al*., 2007; Wadsworth *et al*., 2008) and interactions with a range of division proteins (Karimova *et al*., 2005; D'Ulisse *et al*., 2007; Goehring *et al*., 2007; Grenga *et al*., 2010). The extreme C-terminus of the γ domain, while not required for septal localisation, is also needed for function and protein–protein interactions in *E. coli* and *B. subtilis* (Chen *et al*., 2002; Karimova *et al*., 2005; Robson and King, 2006; Goehring *et al*., 2007). Thus, while the α and γ domains of DivIB are not necessary for peptidoglycan binding, they are essential to ensure correct localisation and interaction with the rest of the divisome. Furthermore, the β domain has been shown to be important for interaction with division proteins (Goehring *et al*., 2007; Masson *et al*., 2009; Rowland *et al*., 2010) and for function (Harry *et al*., 1993; Le Gouellec *et al*., 2008). The ability of *S. aureus* DivIB to bind peptidoglycan via the C-terminal region of the β domain (as predicted from alignments with *G. stearothermophilus* DivIB) does not interfere with domains previously reported as important for function in other species.

Several proteins involved in cell division have been previously characterised as containing a peptidoglycan-binding domain. FtsN is a bitopic cell division protein, with only the periplasmic SPOR (Pfam 23)-containing domain essential for function (Dai *et al*., 1996). FtsN has been shown to bind peptidoglycan (Ursinus *et al*., 2004; Muller *et al*., 2007), with the SPOR domain of *E. coli* FtsN sufficient to mediate midcell localisation (Moll and Thanbichler, 2009; Arends *et al*., 2010). Midcell localisation of three *E. coli* proteins, DamX, DedD and RlpA, is also dependent on the presence of a SPOR domain (Gerding *et al*., 2009). PASTA domains (Pfam 03793) are found mainly in Gram-positive species and are present in the C-terminus of high-molecular-weight PBPs (Yeats *et al*., 2002). Crystal structure analysis of *S. pneumoniae* PBP2x in complex with the β-lactam cefuroxime indicates that PASTA domains recognise unlinked peptidoglycan through van der Waal's forces (Gordon *et al*., 2000). Three groups recently reported the characterisation of *C. crescentus* DipM, a cell division-specific peptidoglycan hydrolase (Goley *et al*., 2010; Moll *et al*., 2010; Poggio *et al*., 2010). Bioinformatic analysis of DipM revealed presence of LysM domains (Pfam 01476), with removal of these domains markedly impairing recruitment to midcell (Moll *et al*., 2010). LysM domains have also been shown to be present in the cell division-associated protein *E. coli* NlpD (Uehara *et al*., 2010), and the SOS-inducible division inhibitors *Mycobacterium tuberculosis* Rv2719c (Chauhan *et al*., 2006) and *B. subtilis* YneA (Mo and Burkholder, 2010). However, *S. aureus* DivIB shows no homology to any peptidoglycan-binding domain previously described for a cell division protein, or indeed to any protein without a recognisable peptidoglycan-binding domain, while structural alignments reveal homology only within the POTRA (α) domain. Therefore, it is likely that DivIB represents a novel class of peptidoglycan-binding protein. This function is conserved, at least among closely related Gram-positive species (this study). The ability of FtsQ to bind peptidoglycan would give insights into the conservation of function among species which have low sequence homology to DivIB of Gram-positive species.

Construction of an *S. aureus* conditional-lethal mutation of *divIB* has shown that this gene is essential for growth in this organism. The orthologous *ftsQ* of *E. coli* is also

essential for growth (Begg *et al*., 1980; Carson *et al*., 1991), while *divIB* essentiality studies in the Gram-positives *B. subtilis* and *S. pneumoniae* have found the gene to be dispensable under certain conditions (Beall and Lutkenhaus, 1989; Harry *et al*., 1993; Le Gouellec *et al*., 2008), suggesting some functional redundancy between different organisms.

The ability of EzrA and FtsZ to localise at midcell in the absence of DivIB indicates that DivIB is not involved in the early stages of the division process. However, DivIB-depleted *S. aureus* cells were blocked in progression of the division cycle, showing that while early components of the divisome are recruited in a DivIB-independent manner, the assembly of the complete divisome is needed for the physical act of septum formation. It may be that DivIB is directly or indirectly involved in the regulation of activity of cell wall synthesising proteins, most likely through protein–protein interactions. Extensive studies have also shown that DivIB/FtsQ interacts with many division proteins (e.g. Di Lallo *et al*., 2003; Buddelmeijer and Beckwith, 2004; Karimova *et al*., 2005; Noirclerc-Savoye *et al*., 2005; Steele *et al*., 2011). Further investigation is needed to fully understand the importance of DivIB interactions with divisome components in regulating cell wall metabolism.

Interestingly, in large DivIB-depleted cells Z-ring diameter was apparently equivalent to the cell diameter, indicating FtsZ constriction did not occur without septum formation. Using membrane-targeted FtsZ in an *in vitro* liposome system it has been shown that Z-rings can undergo constriction in the absence of any other protein (Osawa *et al*., 2008). However, complete division of liposomes was not observed, indicating that while FtsZ alone is sufficient for Z-ring formation and initiation of constriction, a component(s) of the divisome is required for completion of septation.

While *S. aureus* DivIB is not required for recruitment of early division proteins, it was found that GpsB localises in a DivIB-dependent manner, indicating a possible hierarchy of midcell assembly of *S. aureus* division proteins with GpsB being a late recruited protein. *E. coli* FtsQ is required for FtsI (Pbp3) localisation (Weiss *et al*., 1999), while there are strong interdependencies between DivIB, DivIC and FtsL for their recruitment to the division site (Daniel *et al*., 1998; Daniel and Errington, 2000). It has been suggested that GpsB midcell recruitment may be dependent on DivIB/DivIC/FtsL/Pbp2B in *B. subtilis* (Tavares *et al*., 2008), although no interaction has been observed between DivIB and GpsB in *S. aureus* (Steele *et al*., 2011). Thus, requirement of DivIB for GpsB localisation may be through indirect interactions with another component(s) of the divisome.

Although cell division has been studied for many decades, the role of late division proteins in septum formation are still poorly understood. In this study we have shown that in *S. aureus* the septum appears to be formed in two stages with DivIB-independent synthesis of a large ring or 'band' of peptidoglycan equivalent to the diameter of the dividing cell, followed by completion of the septum, which requires DivIB. In ovococci such as *S. pneumoniae*, two types of division-specific cell wall synthesis have been previously described, with synthesis of peripheral cell wall occurring prior to septum formation. Isolation of temperature-sensitive mutants or treatment of ovococci with division-inhibiting concentrations of antibiotics results in filamentation of cells (Higgins *et al*., 1974; Gibson *et al*., 1983; Lleo *et al*., 1990), indicating some longitudinal growth in the absence of septation and suggesting a model of cell wall synthesis with similarities to that reported for rod-shaped bacteria. *S. aureus* only undergoes a single mode of peptidoglycan synthesis (Pinho and Errington, 2003). Thus, to our knowledge this is the first example of a true coccus which undergoes two phases of division-specific cell wall synthesis.

Recent AFM analysis of purified *S. aureus* sacculi has found the peptidoglycan architecture to be comprised of a thickening of peptidoglycan, described as a 'piecrust' at the site of the presumptive septum (Turner *et al*., 2010). After division, this structure remains as orthogonal 'ribs', marking the location of previous division planes. The initial ring of peptidoglycan synthesis observed in DivIB-depleted *S. aureus* correlates to the cell wall piecrust which may act as a buttress to stabilise the cell wall during the remodelling process to form the new septum. A similar phenomenon has been observed indirectly in *S. aureus* cells depleted of PBP1, with depleted cells showing signs of initiation of septation but only a small percentage with completed septa (Pereira *et al*., 2007). This observation appears to be specific for PBP1, as PBP2-depleted cells are not affected in formation of septa, although are affected in septum placement (Pinho *et al*., 2001), while PBP3-deleted *S. aureus* shows no morphological defects (Pinho *et al*., 2000). Thus, DivIB may act in concert with PBP1 to ensure correct formation of septum through either direct interaction with PBP1 or its substrate to regulate enzymatic activity and/or by indirect interactions with other components of the *S. aureus* divisome.

Based on the results presented in this study, we propose that DivIB is required for a morphological checkpoint for the completion of septum formation in *S. aureus*. The divisome assembles at midcell through direct interactions; FtsZ, EzrA and probably the PBPs are recruited independently of DivIB, although some DivIB is likely recruited, perhaps in an inactive form, based on previous interaction studies (Steele *et al*., 2011). Assembly of these proteins at midcell is sufficient to initiate septation, resulting in the formation of the piecrust, a thick band of peptidoglycan that has been suggested to act as a brace to allow dividing cells to withstand changes in cell pressure during hydrolytic

growth of the nascent septal peptidoglycan (Turner *et al.*, 2010). In DivIB-depleted cells, the piecrust was formed but progression of septum completion was blocked, suggesting that DivIB acts as a checkpoint to stop cells undergoing hydrolytic growth, leading to eventual lysis, in the absence of completed septa. Initiation of septum completion may occur through direct interactions of DivIB with the piecrust, and/or with DivIB acting as a molecular connector for the recruitment and assembly of early and later division proteins (such as GpsB), to allow septum completion. It should be noted that DivIC and/or FtsL may also be required for this function, although this could not be established during this study. The misplacement of septa in DivIB-depleted cells also implies that DivIB may play a role in correct septum placement, perhaps through recognition of the piecrust peptidoglycan architecture that marks previous division planes. It could be speculated that the localisation pattern observed for YFP-DivIB in this study correlates to accumulation of DivIB at specific peptidoglycan architectures: after division the thick band of peptidoglycan (piecrust) that is present during septum formation remains as orthogonal ribs, marking the location of previous division planes. The peptidoglycan ribs remain as half or quarter ribs in subsequent divisions due to each daughter cell inheriting an old cell pole from previous rounds of division (Turner *et al.*, 2010). Localisation of DivIB on piecrusts and ribs would result in discrete foci or a line pattern, depending on the orientation and the Z plane sectioning through the cell. Interestingly, DivIB localisation in *S. pneumoniae* was restricted to old hemispheres immediately after division rather than future division sites (Noirclerc-Savoye *et al.*, 2005), suggesting a difference in old and nascent peptidoglycan structure and/or architecture that is specifically recognised by DivIB. It has also been recently shown that *Shigella flexneri* FtsQ is required for the localisation of the IcsA autotransporter at the cell poles, and that the extracytoplasmic domain of FtsQ is required for this localisation (Fixen *et al.*, 2012), further implying a role for DivIB/FtsQ in correct localisation of protein complexes within the cell, perhaps through direct recognition of specific cell wall features.

Thus, work in this study has revealed that DivIB is an important component of the bacterial divisome. Furthermore, investigation of the role of conserved division proteins in organisms of different cellular morphologies provides a useful tool to determine the morphological checkpoints during septation.

Experimental procedures

Bacterial strains, plasmids, and oligonucleotides

The bacterial strains and plasmids used in this study are shown in Table 1, while oligonucleotide sequences used are shown in Table 2.

Growth conditions and media

Escherichia coli, *B. subtilis* and *S. aureus* strains were grown in Luria–Bertani broth (LB; Oxoid), nutrient broth (NB; Oxoid) or brain heart infusion broth (BHI; Oxoid), respectively, at 37°C unless otherwise stated. For growth on solid media, 1.5% (w/v) agar was added. When necessary, the medium was supplemented with erythromycin (5 μg ml^{-1}), chloramphenicol (30 μg ml^{-1}), tetracycline (5 μg ml^{-1}), ampicillin (100 μg ml^{-1}), kanamycin (50 μg ml^{-1}), spectinomycin (100 μg ml^{-1}), 5-bromo-4-chloro-3-indolyl β-D-thiogalactopyranoside (X-Gal, 80 μg ml^{-1}) or isopropyl β-D-thiogalactopyranoside (IPTG, 1 mM).

Transformations of *S. aureus* RN4220 were carried out as previously described (Schenk and Laddaga, 1992). Phage transductions of *S. aureus* using Φ11 were carried out as described by Novick and Morse (1967). General DNA manipulation and transformation of *E. coli* was performed using the method of Sambrook and Russell (2001).

Construction of an S. aureus *divIB-inducible strain*

Attempts to make a DivIB null mutant were carried out using the thermosensitive plasmid pMAD (Arnaud *et al.*, 2004). PCR fragments containing ~ 1 kb flanking regions of *divIB* were amplified from genomic DNA of SH1000 using primers ALB27/ALB28 and ALB29/ALB30 which encoded an internal KpnI restriction site to allow in-frame fusion of the upstream and downstream regions. After KpnI digestion and ligation of the two PCR products the resulting DNA fragment underwent a second PCR reaction using primers ALB27/ALB30. This resulting DNA fragment was digested with BamHI and EcoRI and cloned into pMAD to create pALB29. The plasmid was electroporated into RN4220 at 30°C and subsequently transduced into SH1000 to produce strain ALB16. Several attempts were carried out to isolate a colony in which the deletion of *divIB* was completed due to a two-step homologous recombination event by passaging of ALB16 at 42°C. However, only a single-crossover event, resulting in the integration of pALB29 into the chromosome, was achieved. Deletion of genes by two-step homologous recombination of pMAD relies of the assumption that deletion of the target gene does not affect cell viability. To ensure resolution of pALB29 from the chromosome was not being hindered by the essentiality of *divIB* for cell growth, a chromosomal ectopic copy of *divIB* under the control of P_{Spac} was introduced to allow inducible expression of *divIB* during growth at the permissive temperature. The DNA fragment corresponding to the RBS and coding region of *divIB* under the control of P_{Spac} was PCR amplified from pALB21 using primers ALB127/ALB128. The PCR product was digested with SmaI and BamHI and cloned into pCL84 (Lee *et al.*, 1991). The resulting plasmid, pALB49, was transformed into RN4220 containing pCL112Δ19, a constitutively expressed multi-copy plasmid containing the integrase gene without the *att*P site (Lee *et al.*, 1991). Correct integration of the plasmid into the chromosome was verified by PCR using primers ALB127/ALB128 and by disruption of lipase production on Baird-Parker medium (Oxoid). The chromosomal region, including the plasmid insertion, was then transferred to ALB16 via ϕ11 transduction at 30°C. The

Table 1. Plasmids and bacterial strains used in this study.

	Relevant genotype/markers	Source
Plasmid		
pMAD	*E. coli-S. aureus* shuttle vector with temperature-sensitive origin of replication in *S. aureus* and promoterless *bgaB*; (Amp^r, Ery^r)	Arnaud *et al.* (2004)
pCL84	*S. aureus* recombination vector with attP site of L54a; (Spec^r, Tet^r)	Lee *et al.* (1991)
pGL485	Chloramphenicol-resistant derivative of pMJ8426; (Spec^r, Cam^r)	Cooper *et al.* (2009)
pGL601	pET-21d SaDivIB; (Amp^r)	This study
pGL617	pMUTIN-GFP+ *divIC*; (Amp^r, Ery^r)	This study
pALB17	pET-21d Saβγ; (Amp^r)	This study
pALB18	pET-21d Saβ; (Amp^r)	This study
pALB21	pAISH1 carrying a 1349 bp fragment containing RBS and coding region of *S. aureus divIB*; (Amp^r, Tet^r)	This study
pALB22	pAISH1 carrying an 803 bp fragment containing RBS and 5′ region of *S. aureus DivIB*; (Amp^r, Tet^r)	This study
pALB23	pET-21d BsDivIB; (Amp^r)	This study
pALB29	pMAD containing a 0.95 Kb fragment of the upstream region of *S. aureus divIB* fused in frame to a 1.2 Kb fragment of the downstream region of *S. aureus divIB*; (Amp^r, Ery^r)	This study
pALB34	pET-21d Saβγ Δ263–279; (Amp^r)	This study
pALB35	pET-21d Saβγ Δ263–291; (Amp^r)	This study
pALB36	pET-21d Saβγ Δ263–315; (Amp^r)	This study
pALB37	pET-21d Saβγ Δ263–333; (Amp^r)	This study
pALB40	pET-21d Saβ Δ345–372; (Amp^r)	This study
pALB47	pCL84 P_{Spac}-*divIB*; (Spec^r, Tet^r)	This study
pKASBAR-kan	pUC18 containing attP and kan cassette; (Amp^r, Kan^r)	This study
pALB53*	pMUTIN4 *yfp-divIB*; (Amp^r)	This study
pALB54*-kan	pKASBAR-kan P_{spac}-*yfp-divIB*; (Amp^r, Kan^r)	This study
E. coli		
BL21 (DE3)	F$^-$ *ompT hsdS$_B$* (r_B^- m_B^-) *gal dcm lacY1* (DE3)	Lab strain
B. subtilis		
168	*trp*C2	H.Rogers
S. aureus		
RN4220	Restriction deficient transformation recipient	Kreiswirth *et al.* (1983)
CYL316	RN4220 pCL112Δ19; (Cam^r)	Lee *et al.* (1991)
SH1000	Functional *rsbU*$^+$ derivative of 8325-4	Horsburgh *et al.* (2002)
VF17	SH1000 pGL485; (Cam^r)	Steele *et al.* (2011)
VF94	SH1000 *gpsB-GFP+* pGL485; (Ery^r, Cam^r)	Steele *et al.* (2011)
VF104	SH1000 *ezrA-GFP+* pGL485; (Ery^r, Cam^r)	Steele *et al.* (2011)
ALB1	SH1000 *spa::kan atl::ery*; (Kan^r, Ery^r)	This study
ALB2	SH1000 *divIB-gfp*; (Ery^r, Cam^r)	This study
ALB13	SH1000 P_{Spac}-*divIB* pGL485; (Tet^r, Cam^r)	This study
ALB14	SH1000 P_{Spac}-*divIB5′* pGL485; (Tet^r, Cam^r)	This study
ALB16	SH1000 pALB29; (Ery^r)	This study
ALB26	SH1000 *geh*::P_{Spac}-*divI B ΔdivIB*; (Tet^r)	This study
ALB27	SH1000 *geh*::P_{Spac}-*divIBΔdivIB* pGL485; (Tet^r, Cam^r)	This study
ALB28	SH1000 *spa::kan* pGL485; (Kan^r, Cam^r)	This study
ALB29	SH1000 *spa::kan geh*::P_{Spac}-*divIBΔdivIB* pGL485; (Kan^r, Tet^r, Cam^r)	This study
ALB30	SH1000 *ezrA-GFP+ geh*::P_{Spac}-*divIBΔdivIB* pGL485; (Ery^r, Tet^r, Cam^r)	This study
ALB31	SH1000 *gpsB-GFP+ geh*::P_{Spac}-*divIBΔdivIB* pGL485; (Ery^r, Tet^r, Cam^r)	This study
ALB32	SH1000 *spa::kan ezrA-GFP+* pGL485; (Kan^r, Ery^r, Cam^r)	This study
ALB33	SH1000 *spa::kan ezrA-GFP+ geh*::P_{Spac}-*divIBΔdivIB* pGL485; (Kan^r, Ery^r, Tet^r, Cam^r)	This study
ALB26-yfp	SH1000 *geh*::P_{Spac}-yfp-*divIBΔdivIB*; (Kan^r)	This study
AFK5	SH1000 divIC-gfp+ pGL485; (Ery^r, Cam^r)	This study
AFK24	SH1000 *divIC-GFP+ geh*::P_{Spac}-*divIBΔdivIB* pGL485; (Ery^r, Tet^r, Cam^r)	This study

Ery^r, erythromycin resistant; Tet^r, tetracycline resistant; Kan^r, kanamycin resistant; Cam^r, chloramphenicol resistant; Amp^r, ampicillin resistant; Spec^r, spectinomycin resistant.

resulting strain contained pALB29 inserted in the chromosome due to a single-crossover event and P_{Spac}-*divIB* inserted ectopically at lipase. Colonies in which the deletion of *divIB* due to a double-crossover event, resulting in the excision of the integrated plasmid, were then selected by passaging recombinants at 42°C in the absence of erythromycin. Colonies that showed erythromycin sensitivity and were not blue on X-gal were screened by PCR using primers ALB27/ALB30, and deletion of *divIB* was confirmed by Southern blotting to produce strain ALB26. To allow controlled expression of *divIB* from P_{Spac}, pGL485, a multi-copy plasmid carrying *lacI* (Cooper *et al.*, 2009), was introduced into ALB26 by ϕ11 transduction in the presence of 1 mM IPTG to create strain ALB27.

Table 2. Primers used in this study.

Primer	Sequence	
GLUSH341C5′	ATAATACCATGGCTCCACTTAGTAAAATTGCGCATG	*S. aureus divIB* extracytoplasmic domain
GLUSH341C3′	ATAATACTCGAGATTATTCTTACTTGATTGTTTG	*S. aureus divIB* extracytoplasmic domain
GLUSh378C5′	ATAATAGGTACCTGGAGGTGACAAGCAATGAAAAATAAAGTAG	Upstream region of *S. aureus divIC*
GLUSh378C3′	ATAATACGGCCGTTTTTTCGAAGATTTTGAGCTAGACG	Coding region of *S. aureus divIC*
ALB12	ATAATACCATGGCTAATGAAATTATTGCTTTAGTGAAATATAAA	*S. aureus divIB* β domain
ALB14	ATAATACCATGGCTAGGGATAGTTCGGGTAAACTAAAA	*S. aureus divIB* γ domain
ALB15	ATAATACTCGAGTGATAATGATTGTGACATCTGCGG	*S. aureus divIB* β domain
ALB17	ATAATACCATGGCTAGTAAAGTATCAACAATCTCTGTTACA	*B. subtilis divIB* extracytoplasmic domain
ALB18	ATAATACTCGAGATTTTCATCTTCCTTTTTAGCAG	*B. subtilis divIB* extracytoplasmic domain
ALB27	TTTTTTGGATCCCAGAGTTGTCGTCATTCCAGTTAC	Upstream flanking region of *S. aureus divIB*
ALB28	TTTTTTGGTACCAATTCATCTTTATCTTCATTTGATTCTT	Upstream flanking region of *S. aureus divIB*
ALB29	TTTTTTGGTACCAGAATTACAAAGCGTTTTAAACA	Downstream flanking region of *S. aureus divIB*
ALB30	TTTTTTGGCGTGTGAATTCTAACTTTTT	Downstream flanking region of *S. aureus divIB*
ALB95	ATAATACCATGGCTAAAAACAAACAAAGCAGAATTG	Saβγ Δ263–333
ALB96	ATAATACCATGGCTGAAATGACACCTGAAGTTAGACG	Saβγ Δ263–315
ALB97	ATAATACCATGGCTAAAATTAATGATGCACCTGTC	Saβγ Δ263–291
ALB98	ATAATACCATGGCTGAAAATGGTAAATTGCTTAAAGG	Saβγ Δ263–279
ALB99	AAAAAACTCGAGCGTAAACAATTCAATTCTGCTT	Saβ Δ345–372
ALB127	TTTTTTGGATCCCACAGTAGTTCACCACCTTTT	P_{Spac}-*divIB*
ALB128	TTTTTTCCCGGGATCGTTAAGGGATCAACTTT	P_{Spac}-*divIB*
ALB135	GGCAGCGGTATCATCAACAGGCTTA	Upstream of *attP* and *tet* cassette on pCL84 (natural EcoRI site)
ALB136	TTTTTTGCATGCTCCGCATTAAAATCTAGCG	Downstream of *attP* and *tet* cassette on pCL84
kan_for_HindIII	AAAAAAAAGCTTCAGCGAACCATTTGAGG	Coding region of *kan* cassette
kan_rev_HindIII	AAAAAAAAGCTTAATTCCTCGTAGGCGCTCGG	Coding region of *kan* cassette
yfp_for	CAAGCTTATGGTGAGCAAGGGCGAGGAGCTGTTCACCGGGGTGGTGCCC	Coding region of *yfp*
yfp_rev	CCTCGAGCTTGTACAGCTCGTCCATGCCGAGAGTGATCCCGGCGGCGGT	Coding region of *yfp*
ALB139	TTTTTACTCGAGATGGATGATAAAACGAAGAACG	Coding region of *S. aureus divIB*
ALB140	TTTTTTGGATCCTTAATTATTCTTACTTGATTGTTTGTTAA	Coding region of *S. aureus divIB*
ALB141	TTTTTTGAATTCGCGTTTCGGTGATGAAGA	Upstream of P_{spac} and terminators on pMUTIN2

Restriction sites are underlined.

Construction of fluorescent derivatives of S. aureus *DivIB and DivIC*

To create an N-terminal YFP fusion of DivIB, *yfp* was amplified from SU492 (*B. subtilis ftsZ-yfp*) (Feucht and Lewis, 2001) using primers yfp_for and yfp_rev and ligated to *divIB*, which had been amplified from SH1000 genomic DNA using primers ALB139 and ALB140, using an XhoI cut site that had been introduced during PCR amplification. The product was digested with HindIII and BamHI and inserted into pMUTIN4 (Vagner *et al*., 1998) resulting in plasmid pALB53*. A PCR fragment including *yfp-divIB* under control of the Spac promoter was then amplified from pALB53* using primers ALB141 and ALB140. To insert P_{Spac}-*yfp-divIB* ectopically at the lipase gene of the *S. aureus* chromosome, a high copy number of pCL84 (Lee *et al*., 1991) was created by amplifying a DNA fragment containing *attP* and the *tet* cassette from pCL84 using primers ALB135/ALB136 and inserting into pUC18 using SphI and EcoRI cut sites, creating pKASBAR. The *tet* cassette was then removed and replaced with the *kan* cassette by HindII digestion and ligation. The resulting plasmid, pKASBAR-kan, was then digested with EcoRI and BamHI to allow insertion of P_{Spac}-*yfp-divIB* to create plasmid pALB54*-kan.

The resultant plasmid, pALB54*-kan, was firstly electroporated into RN4220 containing pCL112Δ19 (Lee *et al*., 1991) before being transduced into ALB26 (SH1000 *geh::*P_{Spac}*-divIB ΔdivIB*) and kanamycin-resistant/tetracycline-sensitive colonies were selected. The resulting strain, ALB26-yfp (SH1000 *geh::*P_{Spac}*-yfp-divIB ΔdivIB*), expressed an IPTG-inducible single copy of *yfp-divIB*.

To construct a C-terminal GFP fusion of DivIC, *divIC* was amplified from SH1000 using primers GLUSh378C5′ and GLUSh378C3′and ligated into pMUTIN-Gfp+ (Kaltwasser *et al*., 2002). The resulting plasmid, pGL617, was transformed into *S. aureus* RN4220. Integration of the plasmid into the chromosome occurred via a single-crossover event, resulting in *divIC-gfp+* fusion under the control of the native *divIC* promoter and a native copy of *diviC* under the control of P_{Spac}. The plasmid insertion was transferred into VF17 via ϕ11 transduction to create strain AFK5, and into ALB27 to create strain AFK24.

Generation of antibodies

Anti-DivIB and anti-FtsZ polyclonal antibodies were obtained from a rabbit immunised with purified his-tagged recombinant *S. aureus* DivIB and FtsZ (BioServ UK, UK).

Fluorescence imaging

For fluorescence microscopy, cells from a mid-exponential-phase culture were fixed with formaldehyde and glutaraldehyde as previously described (Pinho and Errington, 2003). For phenotypic imaging of IPTG-inducible strains, cells were depleted of the appropriate protein as described in Steele *et al*. (2011) before fixation of cells. Immunofluorescence imaging was carried out as basically described in Pinho and Errington (2003). Permeabilisation of the cell wall was carried out by lysostaphin digestion at a range of concentrations (20–200 ng ml^{-1}) for 1 min. Primary antibodies were used at the following dilutions: rabbit anti-FtsZ at 1:2000 and rabbit anti-DivIB at 1:100. The secondary antibody used was anti-rabbit IgG AlexaFluor 594 conjugate (Invitrogen). Fluorescence images were acquired using an Olympus IX70 deconvolution microscope and SoftWoRx 3.5.0 software (Applied Precision).

Electron microscopy

The DivIB conditional mutant strain (ALB27) was grown with 0.2 mM IPTG until mid-exponential phase. The culture was washed three times with BHI, diluted in pre-warmed BHI to an initial OD_{600} of 0.01 and grown with or without 1 mM IPTG for 2 h. All samples were fixed overnight in ice-cold 3% (v/v) gluteraldehyde in 0.1 M sodium phosphate buffer pH 7.4. Cell pellets were washed twice in the same buffer before post-fixation with 2% (w/v) osmium tetroxide for 1 h. Following a further buffer-wash step, cells were dehydrated using a graded ethanol series. For SEM samples, cells were then air dried from hexamethyldisilazane using a 1:1 mix of ethanol and hexamethyldisilazane, followed by 100% (v/v) hexamethyldisilazane. Once dried, samples were mounted on 12.5 mm stubs, attached with carbon-sticky tabs and coated in Edwards S150B sputter coater with approximately 25 nm gold. Samples were analysed in a Philips XL-20 scanning electron microscope at an accelerating voltage of 20 Kv. For TEM samples, ethanol-dried samples were incubated in propylene oxide before infiltration of the samples was carried out at room temperature overnight using a 1:1 mix of propylene oxide and araldite resin. Samples were then incubated in araldite resin for 8 h before embedding in fresh araldite resin for 48–72 h at 60°C. 0.5 μm sections were cut on a Reichert Ultracut E ultramicrotome and stained with 1% (w/v) Toluidine blue in 1% (w/v) borax. Ultrathin sections (70–90 nm) were then cut as before and stained with 3% uranyl acetate and Reynold's lead citrate before being viewed using a FEI Tecnai transmission electron microscope at an accelerating voltage of 80 Kv. Electron micrographs were taking using a Gatan digital camera.

Preparation of S. aureus *and* B. subtilis *sacculi*

Sacculi were prepared using the method previously described (Turner *et al*., 2010). Briefly, exponentially growing cultures (OD_{600} ~ 0.5) were collected, boiled for 7 min and broken by FastPrep. Broken cells were then suspended in 5% (w/v) SDS and boiled for 25 min. Insoluble material was collected by centrifugation and the pellet was resuspended in 4% (w/v) SDS and subsequently boiled for 15 min. SDS was removed from samples by repeated washing with distilled water. The resulting pellets were then resuspended in Tris-HCl (50 mM pH 7) containing 2 mg ml^{-1} pronase and incubated at 60°C for 90 min, followed by a single dH_2O wash step. To removed teichoic acids, pellets were resuspended in 250 μl hydrofluoric acid and incubated overnight at 4°C, before being washed six times in distilled water. Samples were stored at –20°C.

Atomic force microscopy

AFM was carried out as previously described (Turner *et al*., 2010). A dilution of sacculi were dried onto freshly cleaved

mica and washed three times with Milli-Q water using a stream of nitrogen. Tapping mode with silicon tips in ambient conditions using a Multimode or Dimension AFM with an Extended Nanoscope IIIa controller (Veeco Instruments) was performed. Images were analysed using Gwyddion and ImageJ.

Cell wall binding assays

The ability of DivIB to bind to peptidoglycan was investigated using the method based on Kern *et al.* (2008). Briefly, samples of a total volume of 200 µl, in binding buffer (20 mM sodium citrate pH5 10 mM $MgCl_2$), containing 0.1 mg ml^{-1} protein and different concentrations of peptidoglycan (0.5, 0.25, 0.125 and 0.0625 mg ml^{-1}) were incubated for 2 h at 37°C. Peptidoglycan, and any associated protein, was separated from unbound protein by centrifugation at 14 000 r.p.m. for 10 min before washing twice in buffer (20 mM sodium citrate pH5 10 mM $MgCl_2$). Equal amounts of supernatant and pellet were then separated on an 11% (w/v) SDS-PAGE gel.

To investigate binding of fluorescent protein to purified peptidoglycan, recombinant proteins were firstly labelled with Cy2 bis-reactive dye (GE Healthcare) using the method described in Schlag *et al.* (2010). Unconjugated dye was separated from labelled protein by dialysis against excess 50 mM sodium phosphate 0.5 M NaCl (pH 7.2) before storage of the conjugated protein at –20°C. To investigate the peptidoglycan binding kinetics of Cy2-labelled protein, 0.25 mg ml^{-1} peptidoglycan was incubated with a range of concentrations of Cy2-labelled protein in a final volume of 200 µl in various binding buffers containing 0.05% (v/v) Tween 20 (either 20 mM sodium citrate pH 5, 20 mM potassium phosphate pH 7.2 or 20 mM Tris pH 9.5 ± 10 mM $MgCl_2$) at room temperature for 5 min. Insoluble peptidoglycan and associated protein was removed by centrifugation and the remaining pellet was washed in the appropriate binding buffer to remove non-specifically bound protein. Bound fluorescent protein was released using 200 µl of 10% (w/v) SDS in two SDS wash steps to ensure complete release of all peptidoglycan-bound protein. Cy2-BSA was included as a negative control. Binding was determined by fluorescence measurement at 525 nm using a Victor™ X3 multilabel reader, and the concentration of bound Cy2-labelled protein was calculated.

Acknowledgements

We are grateful to Chris Hill for assistance with electron microscopy, and to Kasia Wacnik and Bartek Salamaga for the construction of pKASBAR. This work was funded by the Biotechnology and Biological Sciences Research Council (Grant BB/H011005/1). The authors declare no conflict of interest.

References

Angert, E.R. (2005) Alternatives to binary fission in bacteria. *Nat Rev Microbiol* **3:** 214–224.

Arends, S.J., Williams, K., Scott, R.J., Rolong, S., Popham, D.L., and Weiss, D.S. (2010) Discovery and characterization of three new *Escherichia coli* septal ring proteins that contain a SPOR domain: DamX, DedD, and RlpA. *J Bacteriol* **192:** 242–255.

Arnaud, M., Chastanet, A., and Debarbouille, M. (2004) New vector for efficient allelic replacement in naturally nontransformable, low-GC-content, gram-positive bacteria. *Appl Environ Microbiol* **70:** 6887–6891.

Atilano, M.L., Pereira, P.M., Yates, J., Reed, P., Veiga, H., Pinho, M.G., and Filipe, S.R. (2010) Teichoic acids are temporal and spatial regulators of peptidoglycan cross-linking in *Staphylococcus aureus*. *Proc Natl Acad Sci USA* **107:** 18991–18996.

Beall, B., and Lutkenhaus, J. (1989) Nucleotide sequence and insertional inactivation of a *Bacillus subtilis* gene that affects cell division, sporulation, and temperature sensitivity. *J Bacteriol* **171:** 6821–6834.

Begg, K.J., Hatfull, G.F., and Donachie, W.D. (1980) Identification of new genes in a cell envelope-cell division gene cluster of *Escherichia coli*: cell division gene *ftsQ*. *J Bacteriol* **144:** 435–437.

Buddelmeijer, N., and Beckwith, J. (2002) Assembly of cell division proteins at the *E. coli* cell center. *Curr Opin Microbiol* **5:** 553–557.

Buddelmeijer, N., and Beckwith, J. (2004) A complex of the *Escherichia coli* cell division proteins FtsL, FtsB and FtsQ forms independently of its localization to the septal region. *Mol Microbiol* **52:** 1315–1327.

Buddelmeijer, N., Aarsman, M.E., Kolk, A.H., Vicente, M., and Nanninga, N. (1998) Localization of cell division protein FtsQ by immunofluorescence microscopy in dividing and nondividing cells of *Escherichia coli*. *J Bacteriol* **180:** 6107–6116.

Buddelmeijer, N., Judson, N., Boyd, D., Mekalanos, J.J., and Beckwith, J. (2002) YgbQ, a cell division protein in *Escherichia coli* and *Vibrio cholerae*, localizes in codependent fashion with FtsL to the division site. *Proc Natl Acad Sci USA* **99:** 6316–6321.

Calamita, H.G., Ehringer, W.D., Koch, A.L., and Doyle, R.J. (2001) Evidence that the cell wall of *Bacillus subtilis* is protonated during respiration. *Proc Natl Acad Sci USA* **98:** 15260–15263.

Carson, M.J., Barondess, J., and Beckwith, J. (1991) The FtsQ protein of *Escherichia coli*: membrane topology, abundance, and cell division phenotypes due to overproduction and insertion mutations. *J Bacteriol* **173:** 2187–2195.

Chaudhuri, R.R., Allen, A.G., Owen, P.J., Shalom, G., Stone, K., Harrison, M., *et al.* (2009) Comprehensive identification of essential *Staphylococcus aureus* genes using Transposon-Mediated Differential Hybridisation (TMDH). *BMC Genomics* **10:** 291.

Chauhan, A., Lofton, H., Maloney, E., Moore, J., Fol, M., Madiraju, M.V., and Rajagopalan, M. (2006) Interference of *Mycobacterium tuberculosis* cell division by Rv2719c, a cell wall hydrolase. *Mol Microbiol* **62:** 132–147.

Chen, J.C., Minev, M., and Beckwith, J. (2002) Analysis of *ftsQ* mutant alleles in *Escherichia coli*: complementation, septal localization, and recruitment of downstream cell division proteins. *J Bacteriol* **184:** 695–705.

Claessen, D., Emmins, R., Hamoen, L.W., Daniel, R.A., Errington, J., and Edwards, D.H. (2008) Control of the cell elongation-division cycle by shuttling of PBP1 protein in *Bacillus subtilis*. *Mol Microbiol* **68:** 1029–1046.

Cooper, E.L., Garcia-Lara, J., and Foster, S.J. (2009) YsxC,

an essential protein in *Staphylococcus aureus* crucial for ribosome assembly/stability. *BMC Microbiol* **9:** 266.

Dai, K., Xu, Y., and Lutkenhaus, J. (1996) Topological characterization of the essential *Escherichia coli* cell division protein FtsN. *J Bacteriol* **178:** 1328–1334.

Daniel, R.A., and Errington, J. (2000) Intrinsic instability of the essential cell division protein FtsL of *Bacillus subtilis* and a role for DivIB protein in FtsL turnover. *Mol Microbiol* **36:** 278–289.

Daniel, R.A., and Errington, J. (2003) Control of cell morphogenesis in bacteria: two distinct ways to make a rod-shaped cell. *Cell* **113:** 767–776.

Daniel, R.A., Harry, E.J., Katis, V.L., Wake, R.G., and Errington, J. (1998) Characterization of the essential cell division gene *ftsL*(*yIID*) of *Bacillus subtilis* and its role in the assembly of the division apparatus. *Mol Microbiol* **29:** 593–604.

Daniel, R.A., Harry, E.J., and Errington, J. (2000) Role of penicillin-binding protein PBP 2B in assembly and functioning of the division machinery of *Bacillus subtilis*. *Mol Microbiol* **35:** 299–311.

Daniel, R.A., Noirot-Gros, M.F., Noirot, P., and Errington, J. (2006) Multiple interactions between the transmembrane division proteins of *Bacillus subtilis* and the role of FtsL instability in divisome assembly. *J Bacteriol* **188:** 7396–7404.

Di Lallo, G., Fagioli, M., Barionovi, D., Ghelardini, P., and Paolozzi, L. (2003) Use of a two-hybrid assay to study the assembly of a complex multicomponent protein machinery: bacterial septosome differentiation. *Microbiology* **149:** 3353–3359.

D'Ulisse, V., Fagioli, M., Ghelardini, P., and Paolozzi, L. (2007) Three functional subdomains of the *Escherichia coli* FtsQ protein are involved in its interaction with the other division proteins. *Microbiology* **153:** 124–138.

Ebersbach, G., Galli, E., Moller-Jensen, J., Lowe, J., and Gerdes, K. (2008) Novel coiled-coil cell division factor ZapB stimulates Z ring assembly and cell division. *Mol Microbiol* **68:** 720–735.

van den Ent, F., Vinkenvleugel, T.M., Ind, A., West, P., Veprintsev, D., Nanninga, N., *et al*. (2008) Structural and mutational analysis of the cell division protein FtsQ. *Mol Microbiol* **68:** 110–123.

Errington, J., Daniel, R.A., and Scheffers, D.J. (2003) Cytokinesis in bacteria. *Microbiol Mol Biol Rev* **67:** 52–65.

Feucht, A., and Lewis, P.J. (2001) Improved plasmid vectors for the production of multiple fluorescent protein fusions in *Bacillus subtilis*. *Gene* **264:** 289–297.

Figge, R.M., Divakaruni, A.V., and Gober, J.W. (2004) MreB, the cell shape-determining bacterial actin homologue, co-ordinates cell wall morphogenesis in *Caulobacter crescentus*. *Mol Microbiol* **51:** 1321–1332.

Fixen, K.R., Janakiraman, A., Garrity, S., Slade, D.J., Gray, A.N., Karahan, N., *et al*. (2012) Genetic reporter system for positioning of proteins at the bacterial pole. *MBio* **3:** e00251-11.

Gamba, P., Veening, J.W., Saunders, N.J., Hamoen, L.W., and Daniel, R.A. (2009) Two-step assembly dynamics of the *Bacillus subtilis* divisome. *J Bacteriol* **191:** 4186–4194.

Gerding, M.A., Liu, B., Bendezu, F.O., Hale, C.A., Bernhardt, T.G., and de Boer, P.A. (2009) Self-enhanced accumulation of FtsN at Division Sites and Roles for Other Proteins with a SPOR domain (DamX, DedD, and RlpA) in *Escherichia coli* cell constriction. *J Bacteriol* **191:** 7383–7401.

Ghigo, J.M., Weiss, D.S., Chen, J.C., Yarrow, J.C., and Beckwith, J. (1999) Localization of FtsL to the *Escherichia coli* septal ring. *Mol Microbiol* **31:** 725–737.

Gibson, C.W., Daneo-Moore, L., and Higgins, M.L. (1983) Cell wall assembly during inhibition of DNA synthesis in *Streptococcus faecium*. *J Bacteriol* **155:** 351–356.

Goehring, N.W., Petrovska, I., Boyd, D., and Beckwith, J. (2007) Mutants, suppressors, and wrinkled colonies: mutant alleles of the cell division gene *ftsQ* point to functional domains in FtsQ and a role for domain 1C of FtsA in divisome assembly. *J Bacteriol* **189:** 633–645.

Goley, E.D., Comolli, L.R., Fero, K.E., Downing, K.H., and Shapiro, L. (2010) DipM links peptidoglycan remodelling to outer membrane organization in *Caulobacter*. *Mol Microbiol* **77:** 56–73.

Goley, E.D., Yeh, Y.C., Hong, S.H., Fero, M.J., Abeliuk, E., McAdams, H.H., and Shapiro, L. (2011) Assembly of the *Caulobacter* cell division machine. *Mol Microbiol* **80:** 1680–1698.

Gordon, E., Mouz, N., Duee, E., and Dideberg, O. (2000) The crystal structure of the penicillin-binding protein 2x from *Streptococcus pneumoniae* and its acyl-enzyme form: implication in drug resistance. *J Mol Biol* **299:** 477–485.

Grenga, L., Guglielmi, G., Melino, S., Ghelardini, P., and Paolozzi, L. (2010) FtsQ interaction mutants: a way to identify new antibacterial targets. *N Biotechnol* **27:** 870–881.

Guzman, L.M., Weiss, D.S., and Beckwith, J. (1997) Domain-swapping analysis of FtsI, FtsL, and FtsQ, bitopic membrane proteins essential for cell division in *Escherichia coli*. *J Bacteriol* **179:** 5094–5103.

Harry, E.J., Stewart, B.J., and Wake, R.G. (1993) Characterization of mutations in *divIB* of *Bacillus subtilis* and cellular localization of the DivIB protein. *Mol Microbiol* **7:** 611–621.

Higgins, M.L., Daneo-Moore, L., Boothby, D., and Shockman, G.D. (1974) Effect of inhibition of deoxyribonucleic acid and protein synthesis on the direction of cell wall growth in *Streptococcus faecalis*. *J Bacteriol* **118:** 681–692.

Horsburgh, M.J., Aish, J.L., White, I.J., Shaw, L., Lithgow, J.K., and Foster, S.J. (2002) sigmaB modulates virulence determinant expression and stress resistance: characterization of a functional *rsbU* strain derived from *Staphylococcus aureus* 8325-4. *J Bacteriol* **184:** 5457–5467.

Ishikawa, S., Kawai, Y., Hiramatsu, K., Kuwano, M., and Ogasawara, N. (2006) A new FtsZ-interacting protein, YlmF, complements the activity of FtsA during progression of cell division in *Bacillus subtilis*. *Mol Microbiol* **60:** 1364–1380.

Jorge, A.M., Hoiczyk, E., Gomes, G.P., and Pinho, M.G. (2011) EzrA contributes to the regulation of cell size in *Staphylococcus aureus*. *PLoS ONE* **6:** e27542.

Kaltwasser, M., Wiegert, T., and Schumann, W. (2002) Construction and application of epitope- and green fluorescent protein-tagging integration vectors for *Bacillus subtilis*. *Appl Environ Microbiol* **68:** 2624–2628.

Karimova, G., Dautin, N., and Ladant, D. (2005) Interaction network among *Escherichia coli* membrane proteins

involved in cell division as revealed by bacterial two-hybrid analysis. *J Bacteriol* **187:** 2233–2243.
Katis, V.L., and Wake, R.G. (1999) Membrane-bound division proteins DivIB and DivIC of *Bacillus subtilis* function solely through their external domains in both vegetative and sporulation division. *J Bacteriol* **181:** 2710–2718.
Kern, T., Hediger, S., Muller, P., Giustini, C., Joris, B., Bougault, C., *et al*. (2008) Toward the characterization of peptidoglycan structure and protein-peptidoglycan interactions by solid-state NMR spectroscopy. *J Am Chem Soc* **130:** 5618–5619.
Kobayashi, K., Ehrlich, S.D., Albertini, A., Amati, G., Andersen, K.K., Arnaud, M., *et al*. (2003) Essential *Bacillus subtilis* genes. *Proc Natl Acad Sci USA* **100:** 4678–4683.
Kreiswirth, B.N., Lofdahl, S., Betley, M.J., O'Reilly, M., Schlievert, P.M., Bergdoll, M.S., and Novick, R.P. (1983) The toxic shock syndrome exotoxin structural gene is not detectably transmitted by a prophage. *Nature* **305:** 709–712.
Le Gouellec, A., Roux, L., Fadda, D., Massidda, O., Vernet, T., and Zapun, A. (2008) Roles of pneumococcal DivIB in cell division. *J Bacteriol* **190:** 4501–4511.
Lee, C.Y., Buranen, S.L., and Ye, Z.H. (1991) Construction of single-copy integration vectors for *Staphylococcus aureus*. *Gene* **103:** 101–105.
Levin, P.A., Kurtser, I.G., and Grossman, A.D. (1999) Identification and characterization of a negative regulator of FtsZ ring formation in *Bacillus subtilis*. *Proc Natl Acad Sci USA* **96:** 9642–9647.
Li, G., and Howard, S.P. (2010) ExeA binds to peptidoglycan and forms a multimer for assembly of the type II secretion apparatus in *Aeromonas hydrophila*. *Mol Microbiol* **76:** 772–781.
Lleo, M.M., Canepari, P., and Satta, G. (1990) Bacterial cell shape regulation: testing of additional predictions unique to the two-competing-sites model for peptidoglycan assembly and isolation of conditional rod-shaped mutants from some wild-type cocci. *J Bacteriol* **172:** 3758–3771.
McCormick, J.R., and Losick, R. (1996) Cell division gene *ftsQ* is required for efficient sporulation but not growth and viability in *Streptomyces coelicolor* A3(2). *J Bacteriol* **178:** 5295–5301.
Margolin, W. (2000) Themes and variations in prokaryotic cell division. *FEMS Microbiol Rev* **24:** 531–548.
Masson, S., Kern, T., Le Gouellec, A., Giustini, C., Simorre, J.P., Callow, P., *et al*. (2009) Central domain of DivIB caps the C-terminal regions of the FtsL/DivIC coiled-coil rod. *J Biol Chem* **284:** 27687–27700.
Mo, A.H., and Burkholder, W.F. (2010) YneA, an SOS-induced inhibitor of cell division in *Bacillus subtilis*, is regulated posttranslationally and requires the transmembrane region for activity. *J Bacteriol* **192:** 3159–3173.
Mohammadi, T., van Dam, V., Sijbrandi, R., Vernet, T., Zapun, A., Bouhss, A., *et al*. (2011) Identification of FtsW as a transporter of lipid-linked cell wall precursors across the membrane. *EMBO J* **30:** 1425–1432.
Moll, A., and Thanbichler, M. (2009) FtsN-like proteins are conserved components of the cell division machinery in proteobacteria. *Mol Microbiol* **72:** 1037–1053.
Moll, A., Schlimpert, S., Briegel, A., Jensen, G.J., and Thanbichler, M. (2010) DipM, a new factor required for peptidoglycan remodelling during cell division in *Caulobacter crescentus*. *Mol Microbiol* **77:** 90–107.
Muller, P., Ewers, C., Bertsche, U., Anstett, M., Kallis, T., Breukink, E., *et al*. (2007) The essential cell division protein FtsN interacts with the murein (peptidoglycan) synthase PBP1B in *Escherichia coli*. *J Biol Chem* **282:** 36394–36402.
Nguyen-Disteche, M., Fraipont, C., Buddelmeijer, N., and Nanninga, N. (1998) The structure and function of *Escherichia coli* penicillin-binding protein 3. *Cell Mol Life Sci* **54:** 309–316.
Noirclerc-Savoye, M., Le Gouellec, A., Morlot, C., Dideberg, O., Vernet, T., and Zapun, A. (2005) *In vitro* reconstitution of a trimeric complex of DivIB, DivIC and FtsL, and their transient co-localization at the division site in *Streptococcus pneumoniae*. *Mol Microbiol* **55:** 413–424.
Novick, R.P., and Morse, S.I. (1967) *In vivo* transmission of drug resistance factors between strains of *Staphylococcus aureus*. *J Exp Med* **125:** 45–59.
van Opijnen, T., Bodi, K.L., and Camilli, A. (2009) Tn-seq: high-throughput parallel sequencing for fitness and genetic interaction studies in microorganisms. *Nat Methods* **6:** 767–772.
Osawa, M., Anderson, D.E., and Erickson, H.P. (2008) Reconstitution of contractile FtsZ rings in liposomes. *Science* **320:** 792–794.
Pereira, S.F., Henriques, A.O., Pinho, M.G., de Lencastre, H., and Tomasz, A. (2007) Role of PBP1 in cell division of *Staphylococcus aureus*. *J Bacteriol* **189:** 3525–3531.
Pinho, M.G., and Errington, J. (2003) Dispersed mode of *Staphylococcus aureus* cell wall synthesis in the absence of the division machinery. *Mol Microbiol* **50:** 871–881.
Pinho, M.G., and Errington, J. (2005) Recruitment of penicillin-binding protein PBP2 to the division site of *Staphylococcus aureus* is dependent on its transpeptidation substrates. *Mol Microbiol* **55:** 799–807.
Pinho, M.G., de Lencastre, H., and Tomasz, A. (2000) Cloning, characterization, and inactivation of the gene *pbpC*, encoding penicillin-binding protein 3 of *Staphylococcus aureus*. *J Bacteriol* **182:** 1074–1079.
Pinho, M.G., Filipe, S.R., de Lencastre, H., and Tomasz, A. (2001) Complementation of the essential peptidoglycan transpeptidase function of penicillin-binding protein 2 (PBP2) by the drug resistance protein PBP2A in *Staphylococcus aureus*. *J Bacteriol* **183:** 6525–6531.
Poggio, S., Takacs, C.N., Vollmer, W., and Jacobs-Wagner, C. (2010) A protein critical for cell constriction in the Gram-negative bacterium *Caulobacter crescentus* localizes at the division site through its peptidoglycan-binding LysM domains. *Mol Microbiol* **77:** 74–89.
Real, G., and Henriques, A.O. (2006) Localization of the *Bacillus subtilis murB* gene within the dcw cluster is important for growth and sporulation. *J Bacteriol* **188:** 1721–1732.
Robson, S.A., and King, G.F. (2006) Domain architecture and structure of the bacterial cell division protein DivIB. *Proc Natl Acad Sci USA* **103:** 6700–6705.
Rowland, S.L., Wadsworth, K.D., Robson, S.A., Robichon, C., Beckwith, J., and King, G.F. (2010) Evidence from artificial septal targeting and site-directed mutagenesis that residues in the extracytoplasmic beta domain of DivIB

mediate its interaction with the divisomal transpeptidase PBP 2B. *J Bacteriol* **192:** 6116–6125.
Sambrook, J., and Russell, D.W. (2001) *Molecular Cloning: A Laboratory Manual*. Cold Spring Harbor, NY: Cold Spring Harbor Laboratory Press.
Sanchez-Pulido, L., Devos, D., Genevrois, S., Vicente, M., and Valencia, A. (2003) POTRA: a conserved domain in the FtsQ family and a class of beta-barrel outer membrane proteins. *Trends Biochem Sci* **28:** 523–526.
Schenk, S., and Laddaga, R.A. (1992) Improved method for electroporation of *Staphylococcus aureus*. *FEMS Microbiol Lett* **73:** 133–138.
Schlag, M., Biswas, R., Krismer, B., Kohler, T., Zoll, S., Yu, W., *et al*. (2010) Role of staphylococcoal wall teichoic acid in targeting the major autolysin Atl. *Mol Microbiol* **75:** 864–873.
Schmidt, K.L., Peterson, N.D., Kustusch, R.J., Wissel, M.C., Graham, B., Phillips, G.J., and Weiss, D.S. (2004) A predicted ABC transporter, FtsEX, is needed for cell division in *Escherichia coli*. *J Bacteriol* **186:** 785–793.
Song, J.H., Ko, K.S., Lee, J.Y., Baek, J.Y., Oh, W.S., Yoon, H.S., *et al*. (2005) Identification of essential genes in *Streptococcus pneumoniae* by allelic replacement mutagenesis. *Mol Cells* **19:** 365–374.
Steele, V.R., Bottomley, A.L., Garcia-Lara, J., Kasturiarachchi, J., and Foster, S.J. (2011) Multiple essential roles for EzrA in cell division of *Staphylococcus aureus*. *Mol Microbiol* **80:** 542–555.
Tavares, J.R., de Souza, R.F., Meira, G.L., and Gueiros-Filho, F.J. (2008) Cytological characterization of YpsB, a novel component of the *Bacillus subtilis* divisome. *J Bacteriol* **190:** 7096–7107.
Thompson, L.S., Beech, P.L., Real, G., Henriques, A.O., and Harry, E.J. (2006) Requirement for the cell division protein DivIB in polar cell division and engulfment during sporulation in *Bacillus subtilis*. *J Bacteriol* **188:** 7677–7685.
Turner, R.D., Ratcliffe, E.C., Wheeler, R., Golestanian, R., Hobbs, J.K., and Foster, S.J. (2010) Peptidoglycan architecture can specify division planes in *Staphylococcus aureus*. *Nat Commun* **1:** 26.
Typas, A., Banzhaf, M., Gross, C.A., and Vollmer, W. (2012) From the regulation of peptidoglycan synthesis to bacterial growth and morphology. *Nat Rev Microbiol* **10:** 123–136.
Uehara, T., Parzych, K.R., Dinh, T., and Bernhardt, T.G. (2010) Daughter cell separation is controlled by cytokinetic ring-activated cell wall hydrolysis. *EMBO J* **29:** 1412–1422.
Ursinus, A., van den Ent, F., Brechtel, S., de Pedro, M., Holtje, J.V., Lowe, J., and Vollmer, W. (2004) Murein (peptidoglycan) binding property of the essential cell division protein FtsN from *Escherichia coli*. *J Bacteriol* **186:** 6728–6737.
Utsui, Y., and Yokota, T. (1985) Role of an altered penicillin-binding protein in methicillin- and cephem-resistant *Staphylococcus aureus*. *Antimicrob Agents Chemother* **28:** 397–403.
Vagner, V., Dervyn, E., and Ehrlich, S.D. (1998) A vector for systematic gene inactivation in *Bacillus subtilis*. *Microbiology* **144:** 3097–3104.
Wadsworth, K.D., Rowland, S.L., Harry, E.J., and King, G.F. (2008) The divisomal protein DivIB contains multiple epitopes that mediate its recruitment to incipient division sites. *Mol Microbiol* **67:** 1143–1155.
Weiss, D.S., Chen, J.C., Ghigo, J.M., Boyd, D., and Beckwith, J. (1999) Localization of FtsI (PBP3) to the septal ring requires its membrane anchor, the Z ring, FtsA, FtsQ, and FtsL. *J Bacteriol* **181:** 508–520.
Yeats, C., Finn, R.D., and Bateman, A. (2002) The PASTA domain: a beta-lactam-binding domain. *Trends Biochem Sci* **27:** 438.

Supporting information

Additional supporting information may be found in the online version of this article at the publisher's web-site.